Head vs Tail Squaramide – Naphthalimide Conjugates: Self Assembly and Anion Binding Behaviour

Anthony A. Abogunrin[1], Stephen Healy[1], Orla Fenelon[1]and Robert B. P. Elmes[1,2,3]*

[1]*Department of Chemistry, Maynooth University, National University of Ireland, Maynooth, Co. Kildare, Ireland.*

Tel: +353 1 7084615; E-mail: robert.elmes@mu.ie

[2] *Synthesis and Solid State Pharmaceutical Centre (SSPC), Ireland.*

[3] *Kathleen Lonsdale Institute for Human Health Research, Maynooth University, National University of Ireland, Maynooth, Co. Kildare, Ireland.*

Supporting Information

^{1}H NMR Anion Binding Studies:

Both the tetrabutylammonium salts and the receptors were lyophilised before use. Solutions of the TBA salts were made up in DMSO-d_6, which was dried over 3Å molecular sieves, to a concentration of 20 mM. An aliquot of stock solution of receptor in DMSO-d_6 was diluted to 1 mL (2.5 mM). 600 μL of this solution was added to an NMR tube and the ^{1}H NMR spectrum was recorded. Subsequent additions of aliquots of TBA salt solutions were added to the NMR tube and shaken vigorously to ensure homogenisation. This process was repeated until up to 20 equivalents of halide was reached. The ^{1}H NMR spectra were analysed and processed, and stackplots were generated using MestReNova 6.0.2 software. A global fitting analysis assuming a 1:1 binding model was employed to provide the binding constant (K_a/M^{-1}), by fitting of the chemical shift changes of the NH signals as function of anion concentration using the open access BindFit software program.

Spectroscopic Binding Studies: Spectroscopic titrations were performed by additions of aliquots of the putative anionic guest as the tetrabutylammonium (TBA) salt solution (20 mM) in DMSO to a solution of the receptor in DMSO. After each addition, the resulting solution was stirred for at least 30 seconds and the UV or fluorescence spectrum was recorded. Both salt and receptor were dried under high vacuum prior to use.

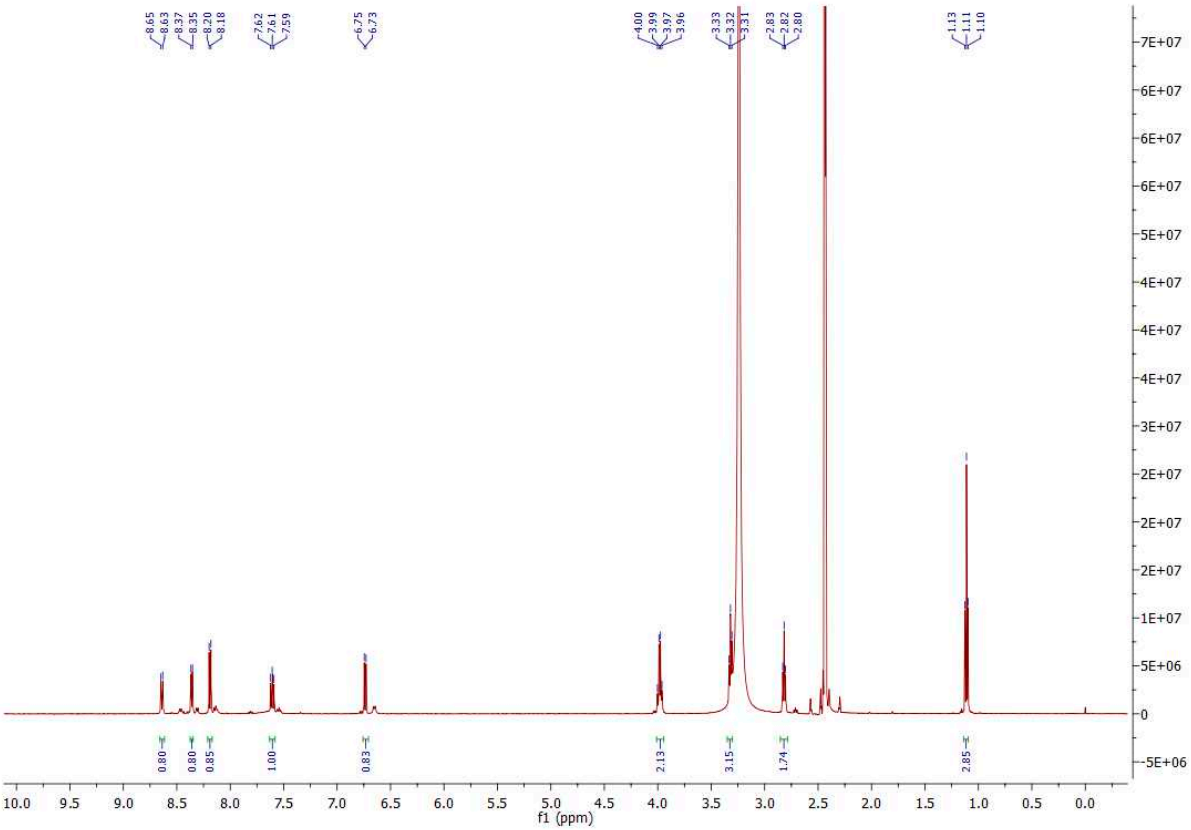

Figure S1. ^{1}H NMR (DMSO-d$_6$, 500 MHz) spectrum of **2.**

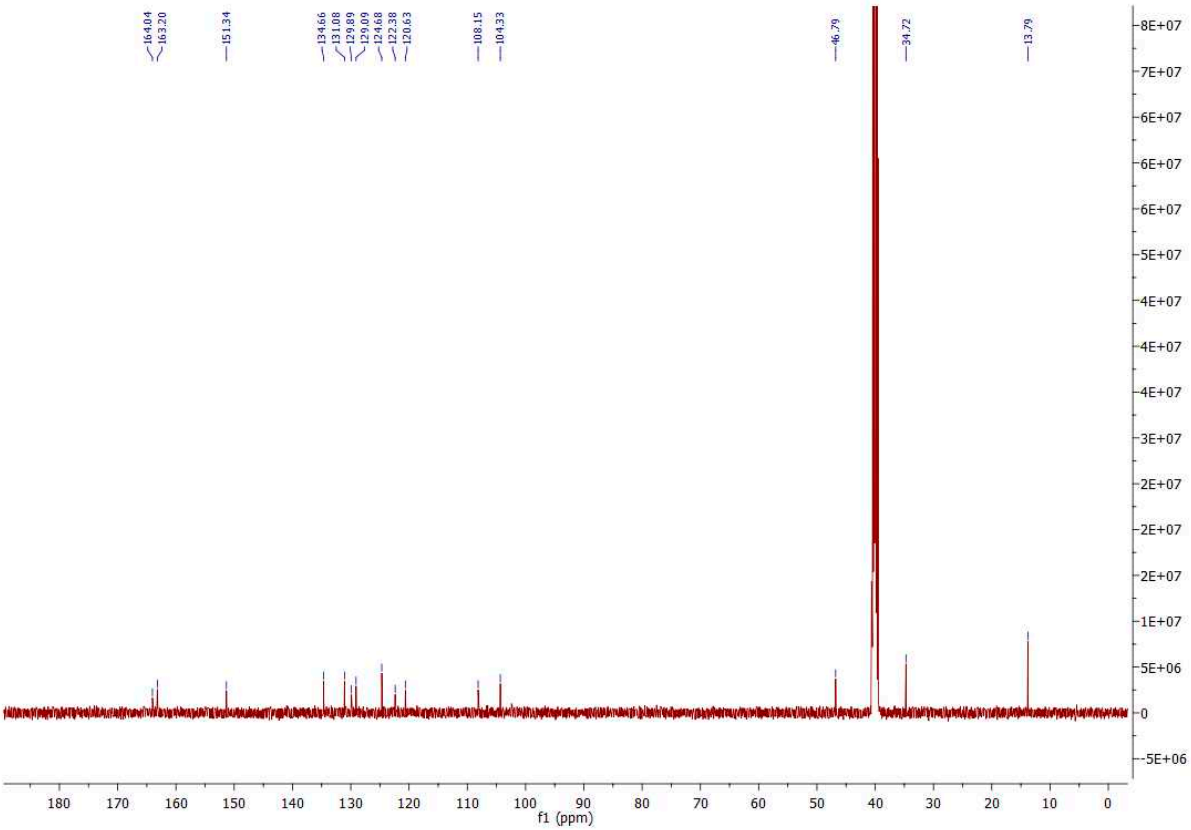

Figure S2. ^{13}C NMR (DMSO-d$_6$, 126 MHz) spectrum of **2.**

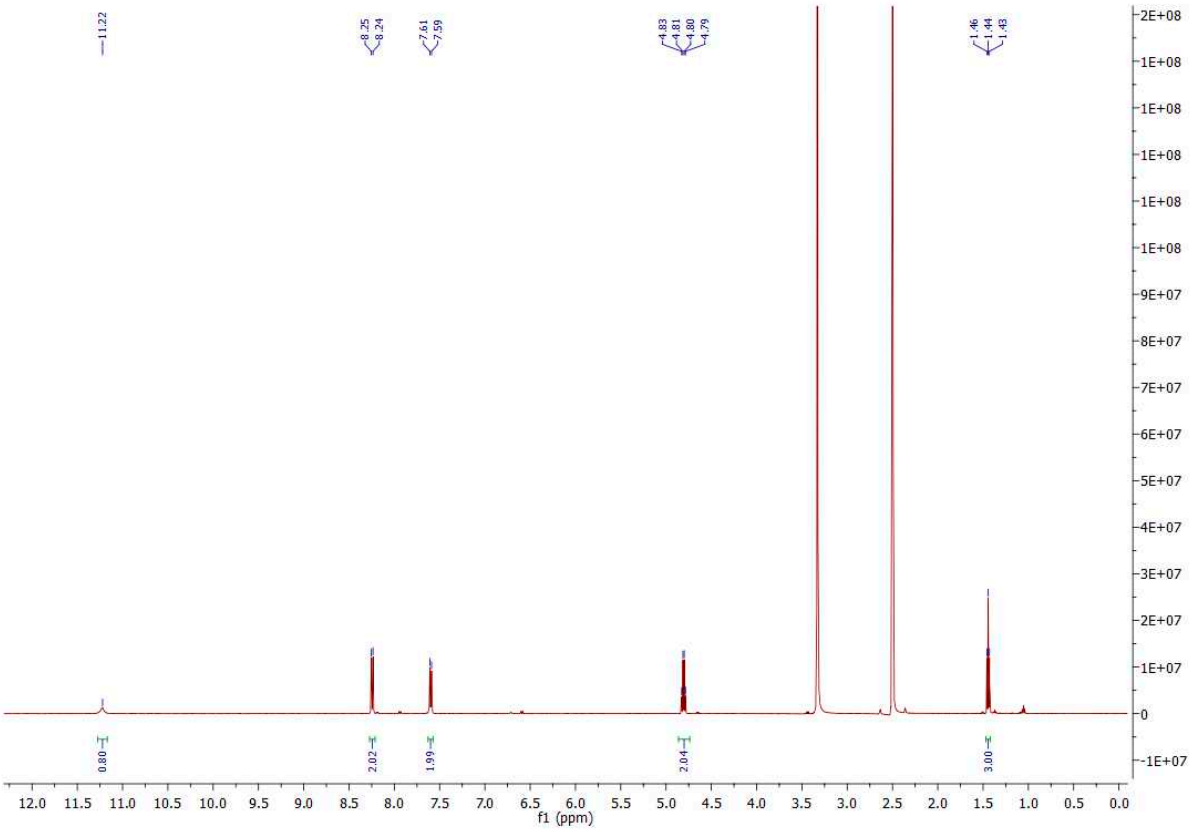

Figure S3. ^{1}H NMR (DMSO-d$_6$, 500 MHz) spectrum of **3.**

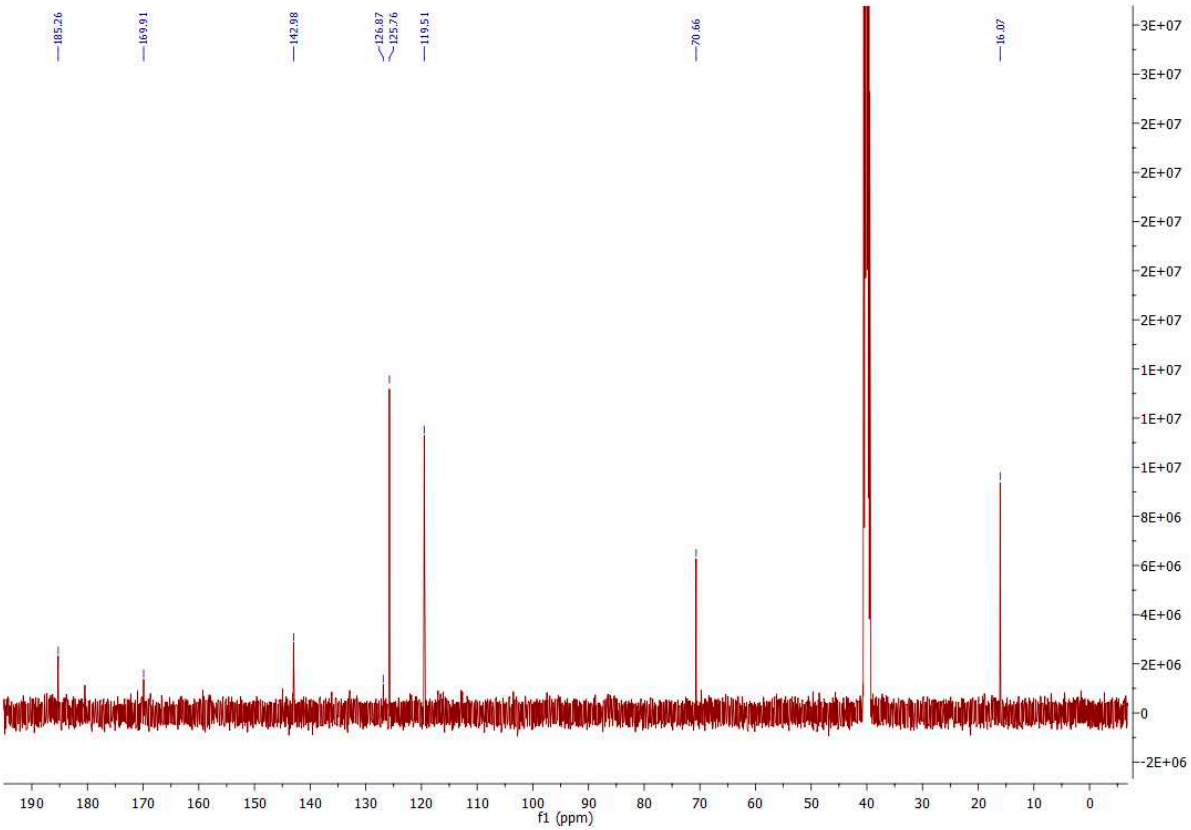

Figure S4. ^{13}C NMR (DMSO-d$_6$, 126 MHz) spectrum of **3.**

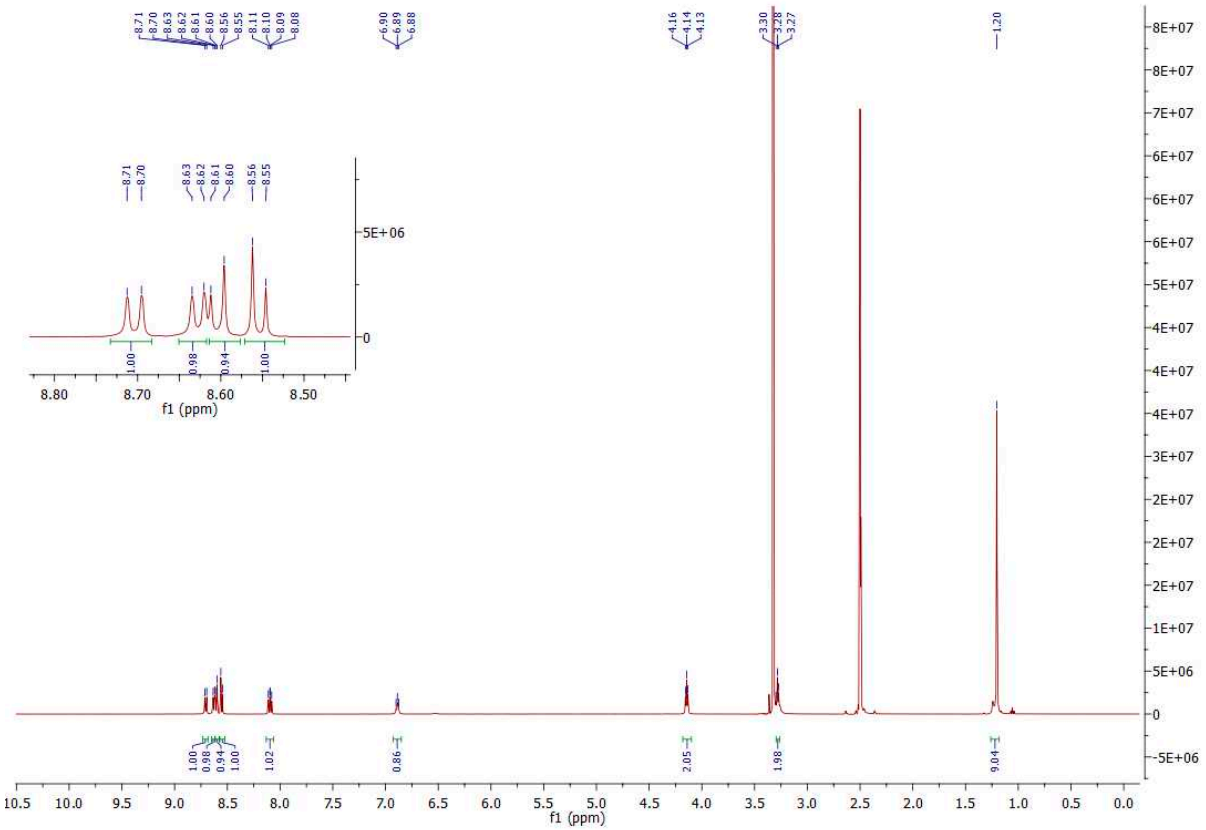

Figure S5. [1]H NMR (DMSO-d$_6$, 500 MHz) spectrum of **5. Inset:** Zoom of the aromatic region.

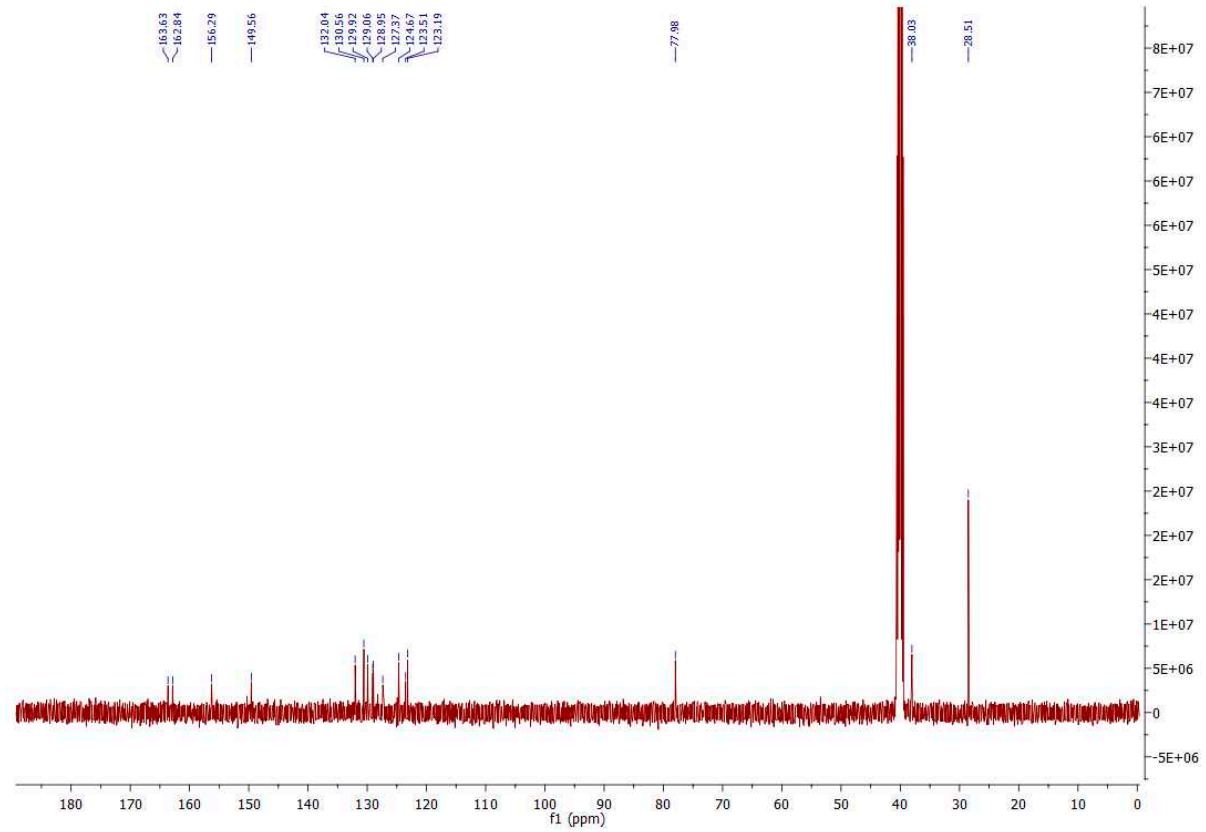

Figure S6. [13]C NMR (DMSO-d$_6$, 126 MHz) spectrum of **5.**

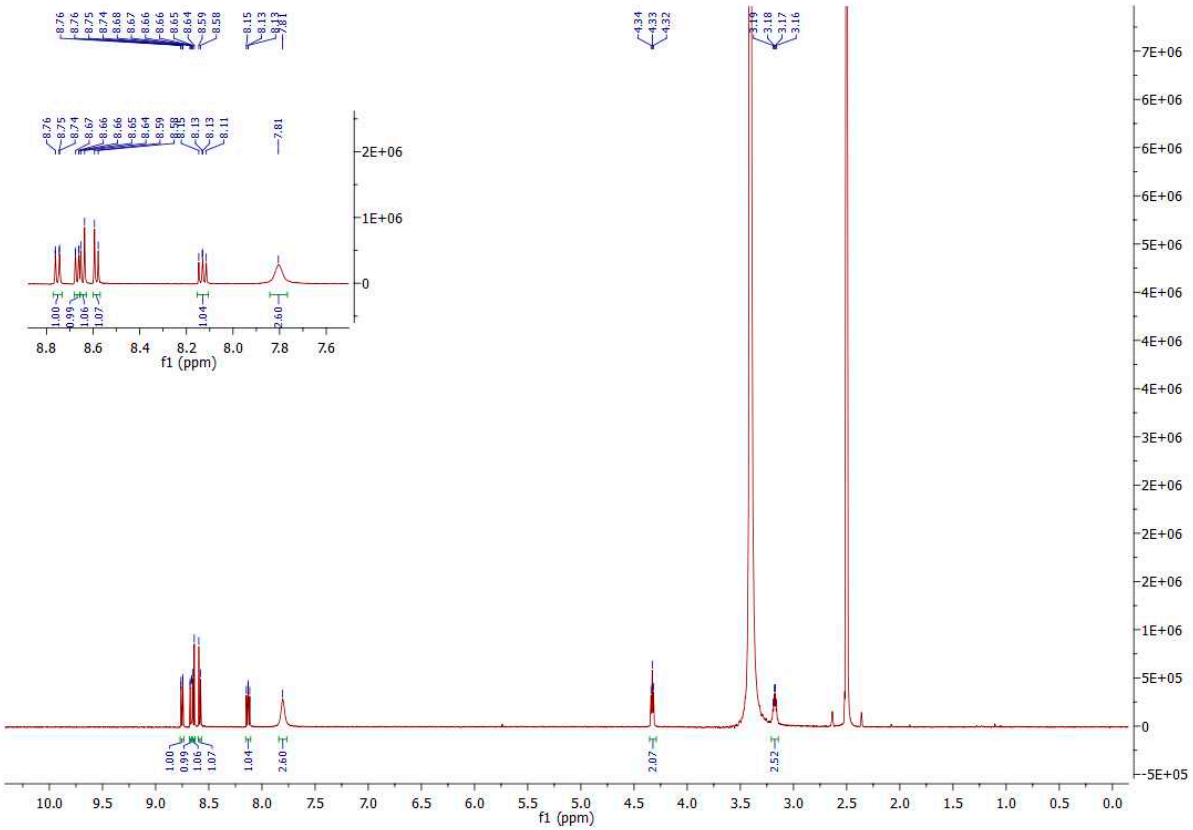

Figure S7. ^{1}H NMR (DMSO-d$_6$, 500 MHz) spectrum of **6. Inset:** Zoom of the aromatic region

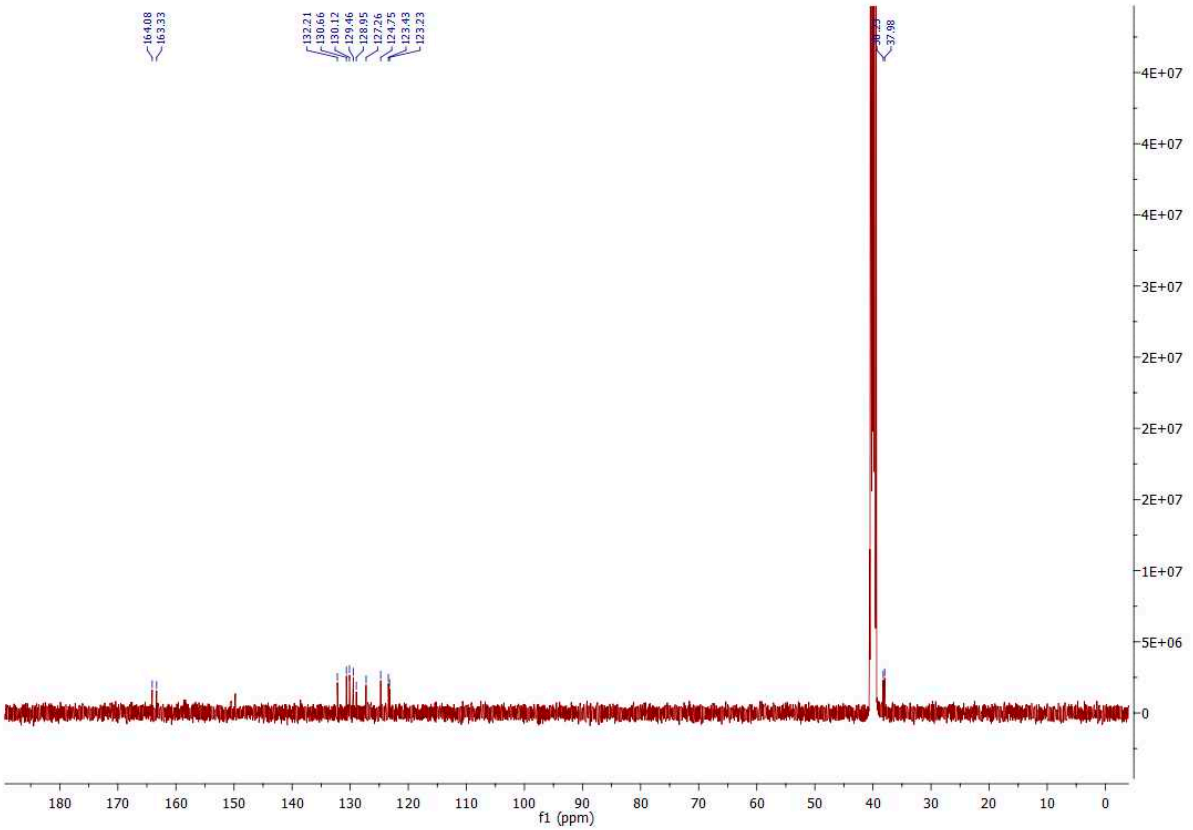

Figure S8. ^{13}C NMR (DMSO-d$_6$, 126 MHz) spectrum of **6.**

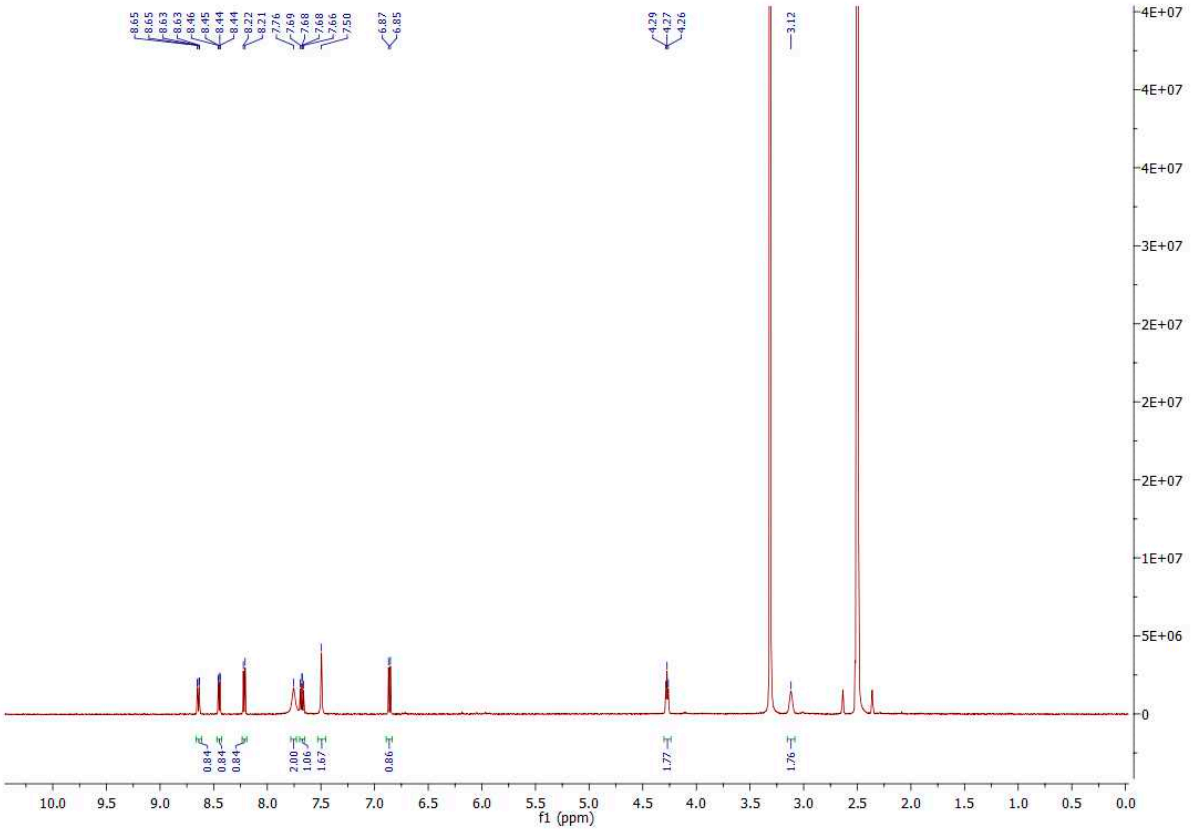

Figure S9. ^{1}H NMR (DMSO-d$_6$, 500 MHz) spectrum of **7.**

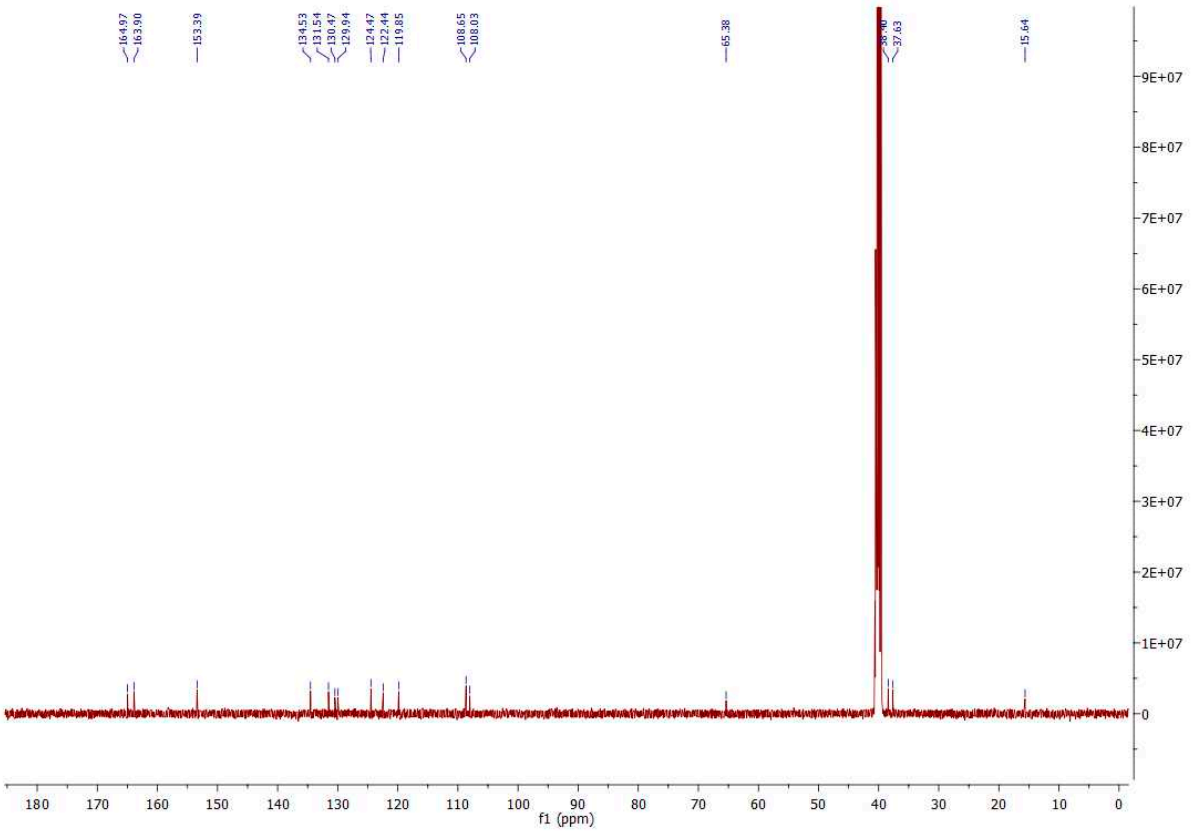

Figure S10. ^{13}C NMR (DMSO-d$_6$, 126 MHz) spectrum of **7.**

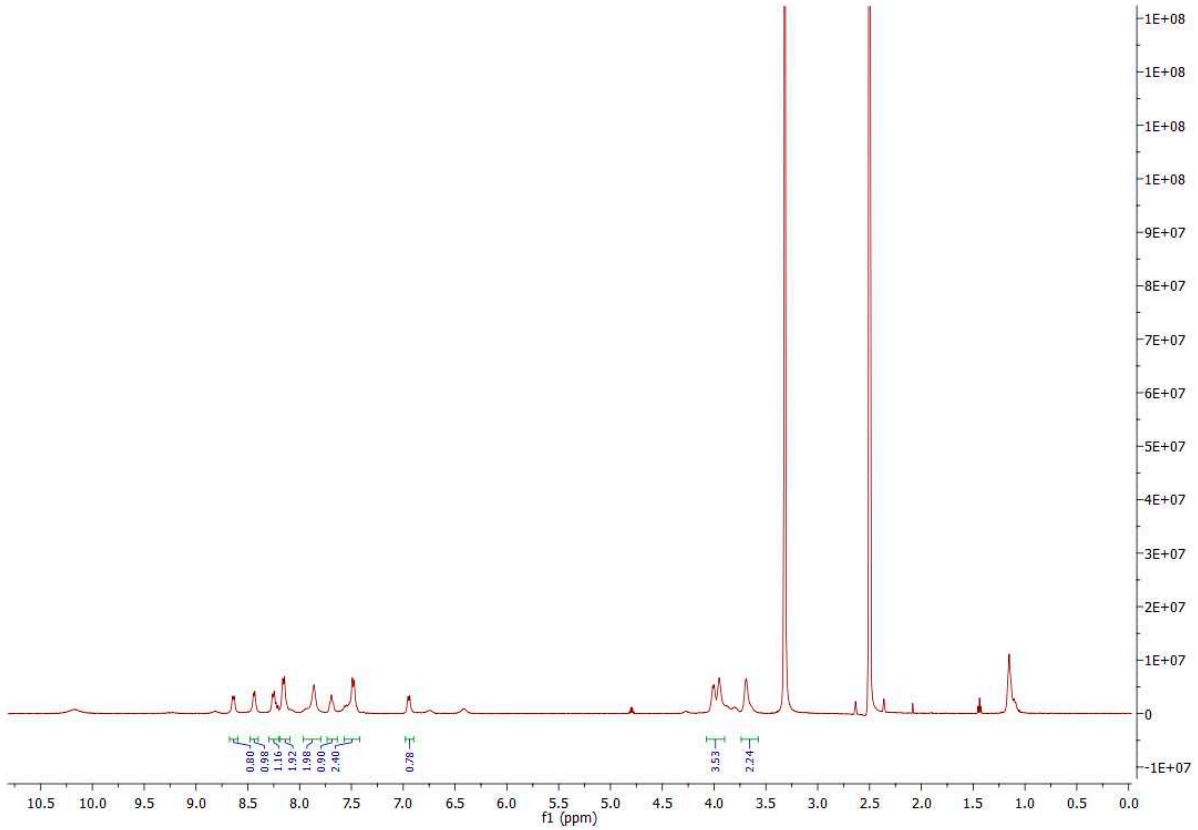

Figure S11. ^{1}H NMR (DMSO-d_6, 500 MHz) spectrum of **SN1** at 293K**.**

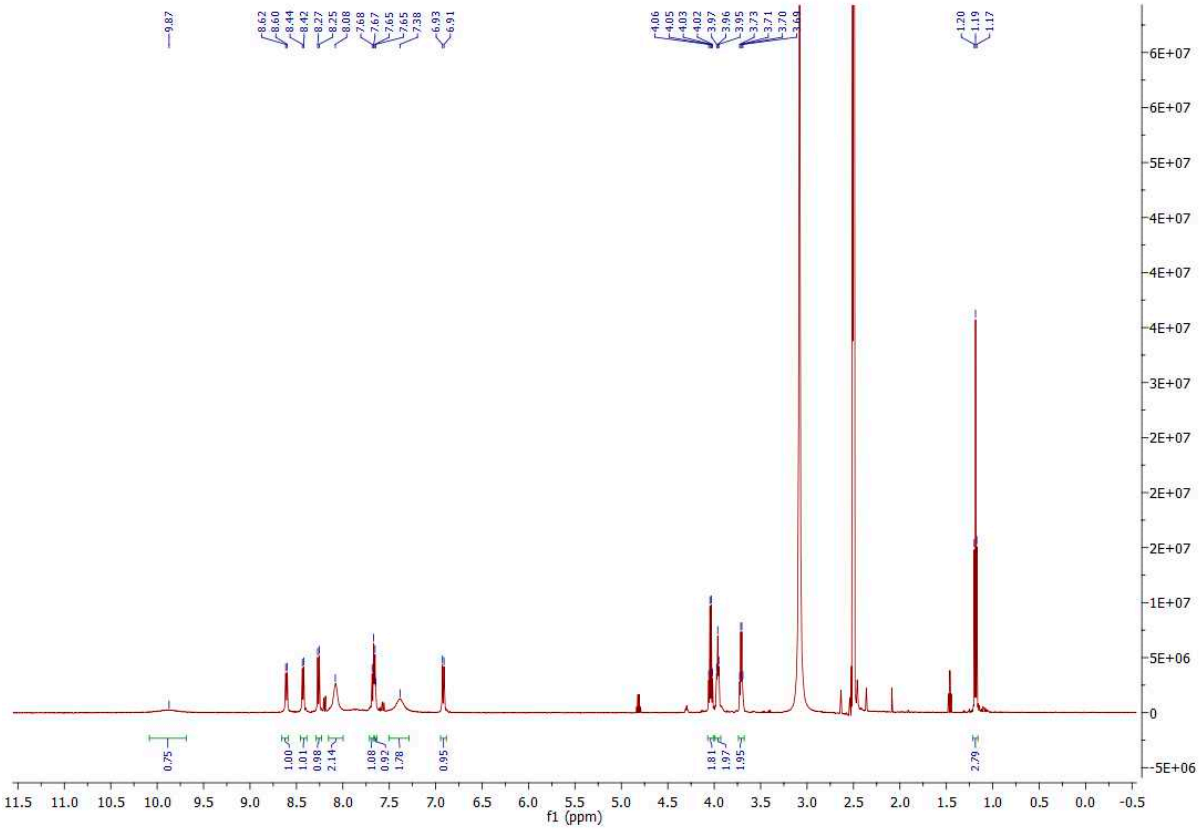

Figure S12. ^{1}H NMR (DMSO-d_6, 500 MHz) spectrum of **SN1** at 343K**.**

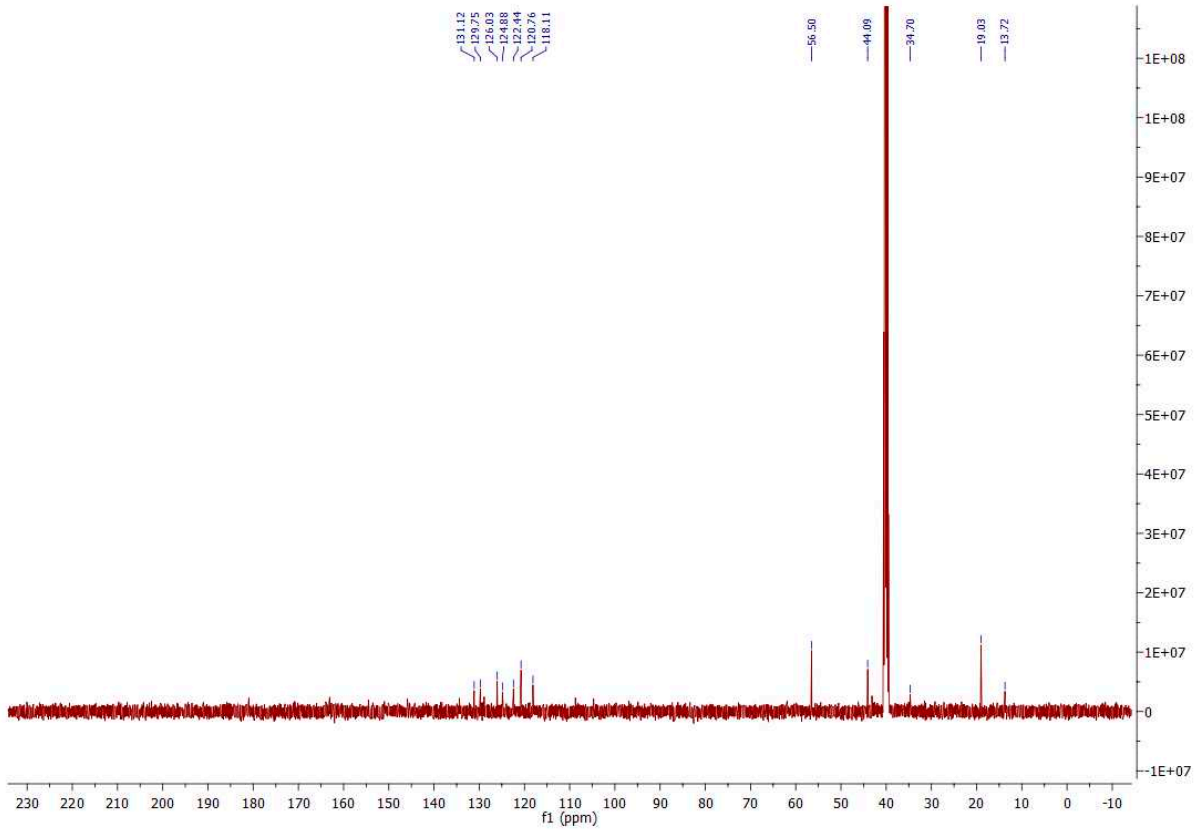

Figure S13. ^{13}C NMR (DMSO-d$_6$, 126 MHz) spectrum of **SN1** at 293K**.**

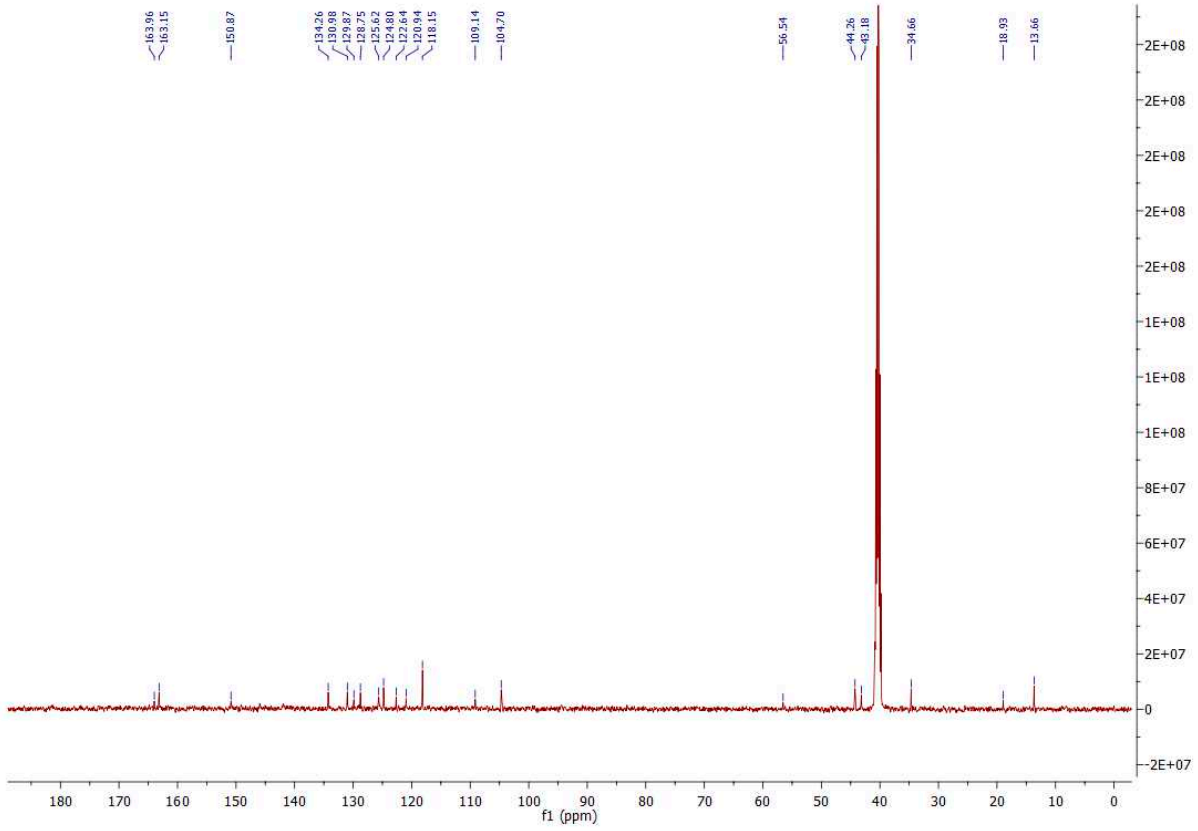

Figure S14. ^{13}C NMR (DMSO-d$_6$, 126 MHz) spectrum of **SN1** at 340K**.**

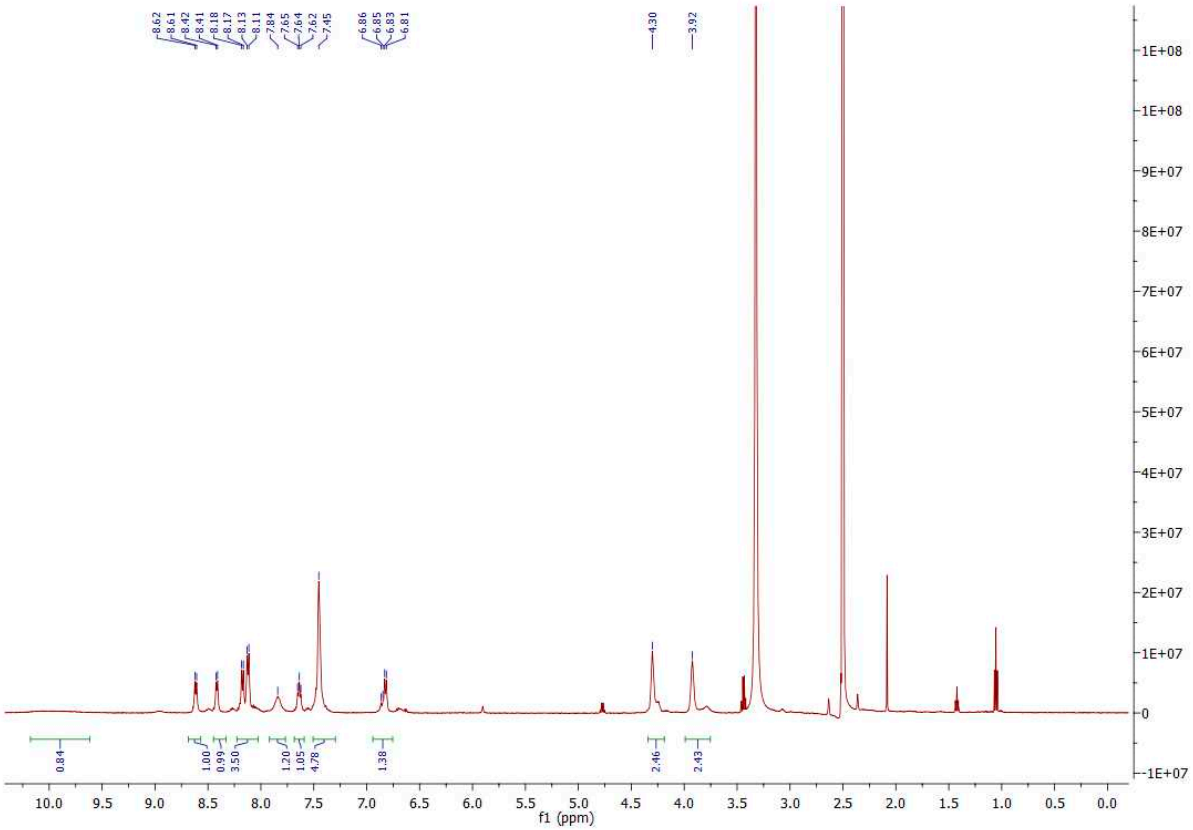

Figure S15. ^{1}H NMR (DMSO-d$_6$, 500 MHz) spectrum of **SN2** at 293K**.**

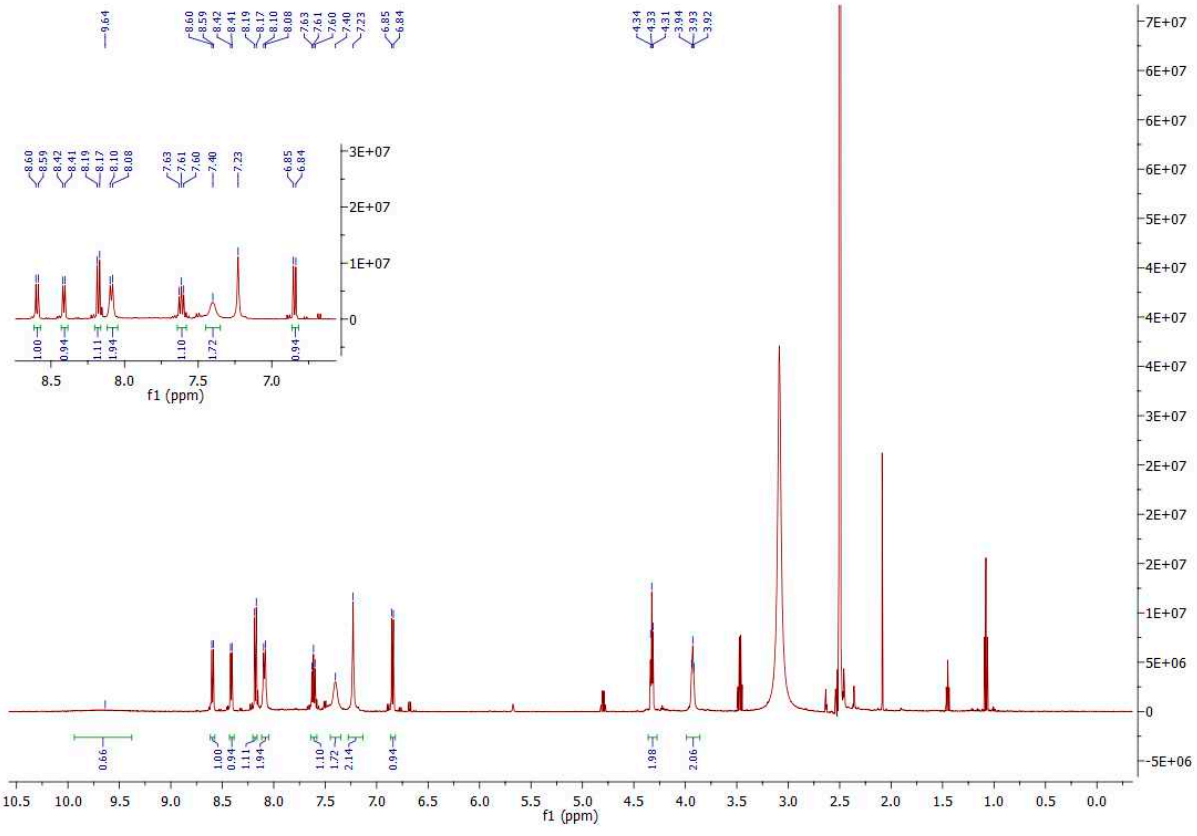

Figure S16. ^{1}H NMR (DMSO-d$_6$, 500 MHz) spectrum of **SN2** at 340K**. Inset:** Zoom of the aromatic region

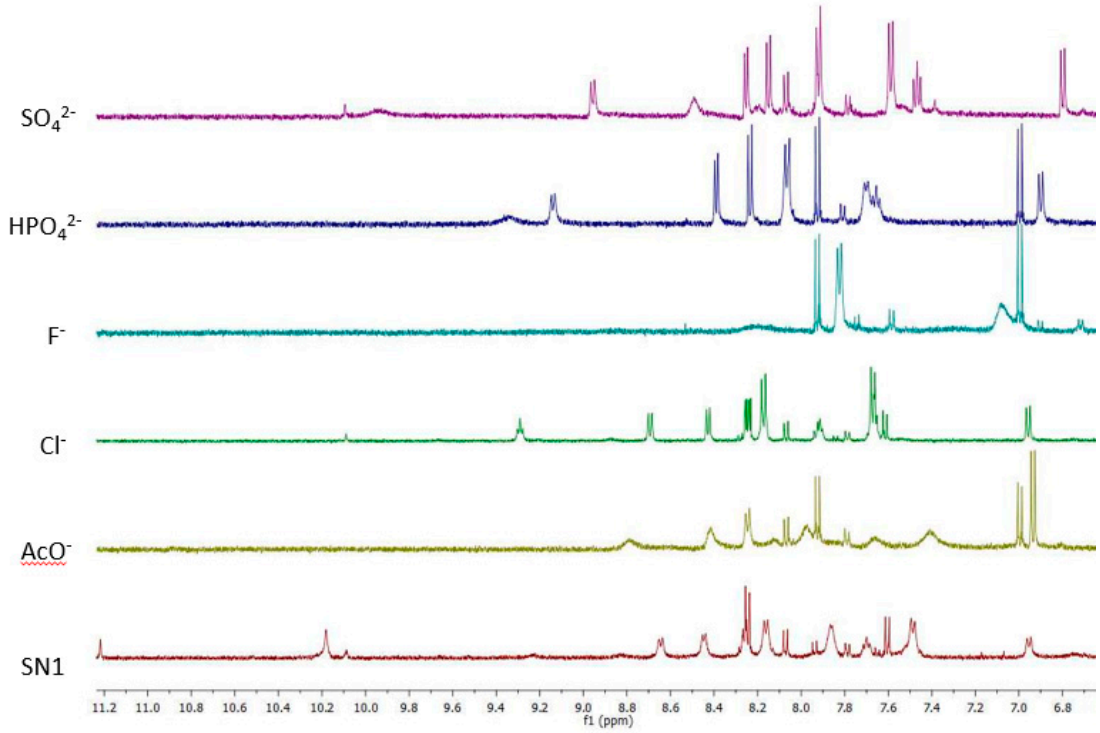

Figure S17: ^{1}H NMR stackplot of **SN1** with various anions (30 equivalents) in 0.5% H_2O in DMSO-d_6 at 298 K.

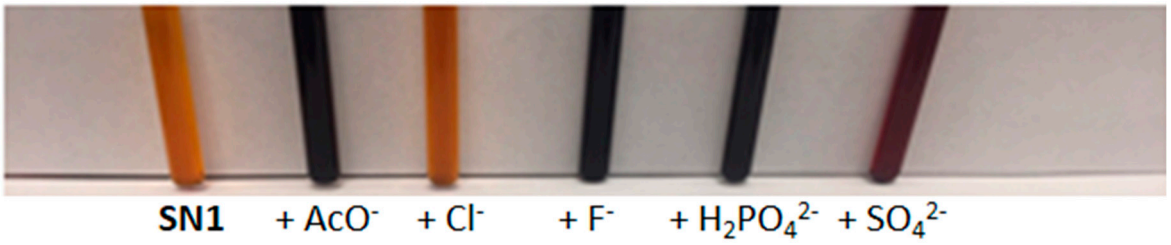

Figure S18: The differing spectroscopic response of compound **SN1** upon the addition 75 µl equivalents of anions as TBA salts in DMSO-d_6 (AcO^-, Cl^-, F^-, HPO_4^{2-}, SO_4^{2-}), with the naked eye.

a)

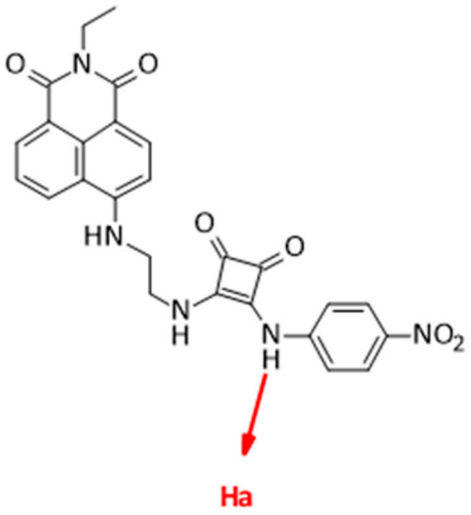

b)

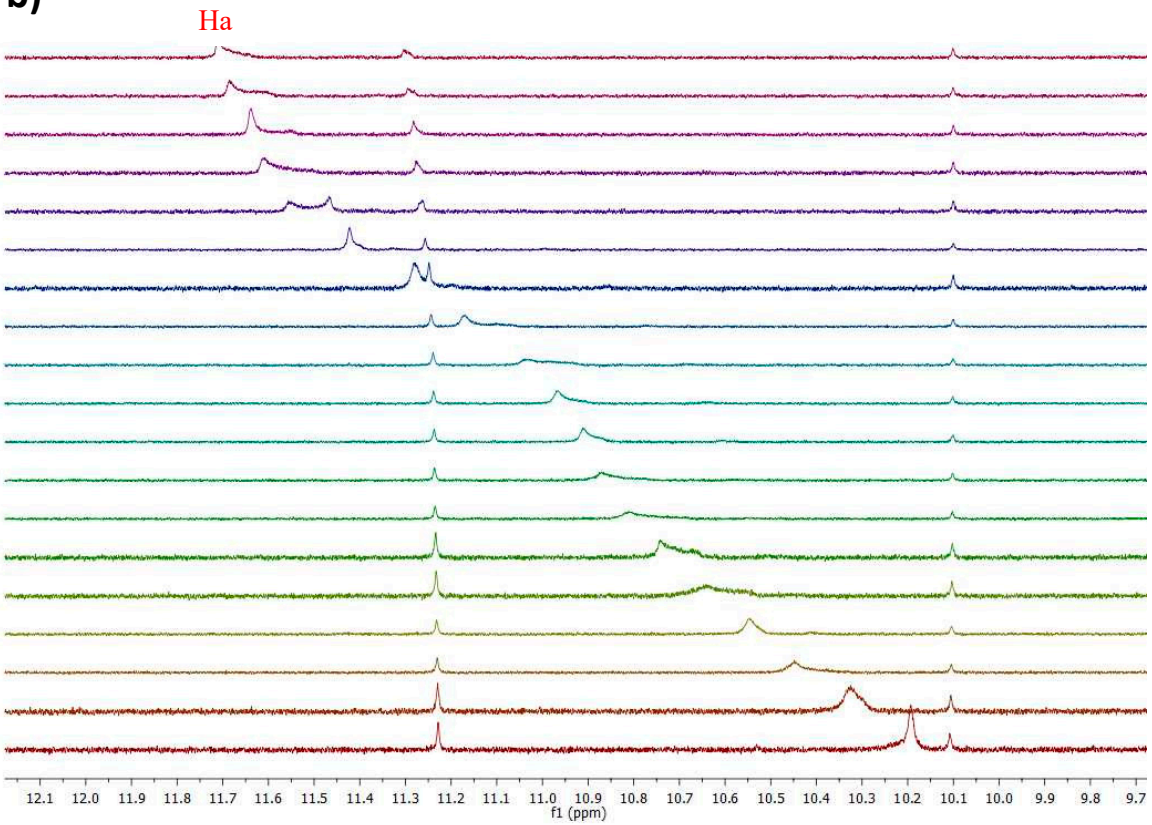

Figure S19: **(a)**: Structure of **SN1** showing the NH proton as Ha. **(b)**: Changes in the ^{1}H NMR spectrum (Ha proton) of **SN1** upon the addition 0 - 20 equivalents of anions as TBA chloride in DMSO-d_6.

(a)

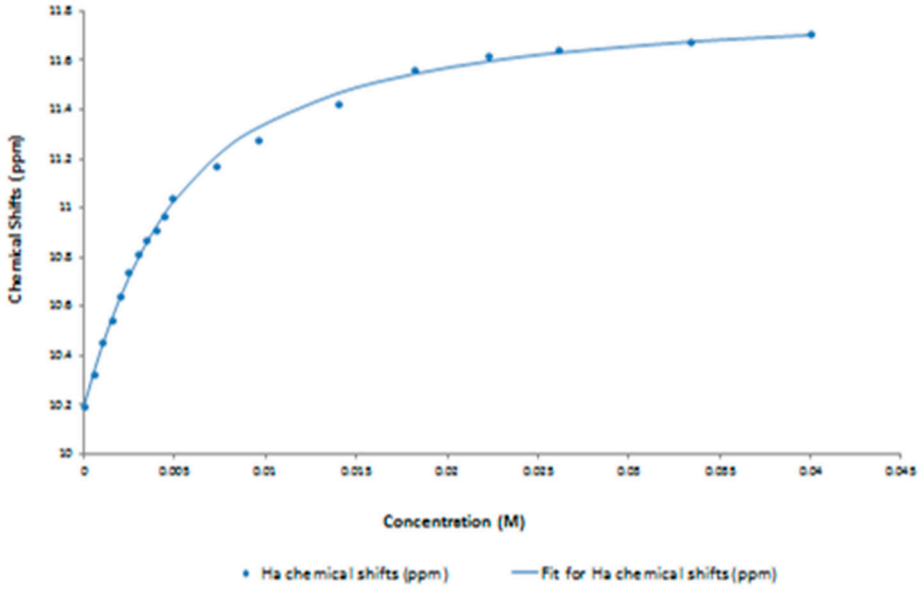

(b)

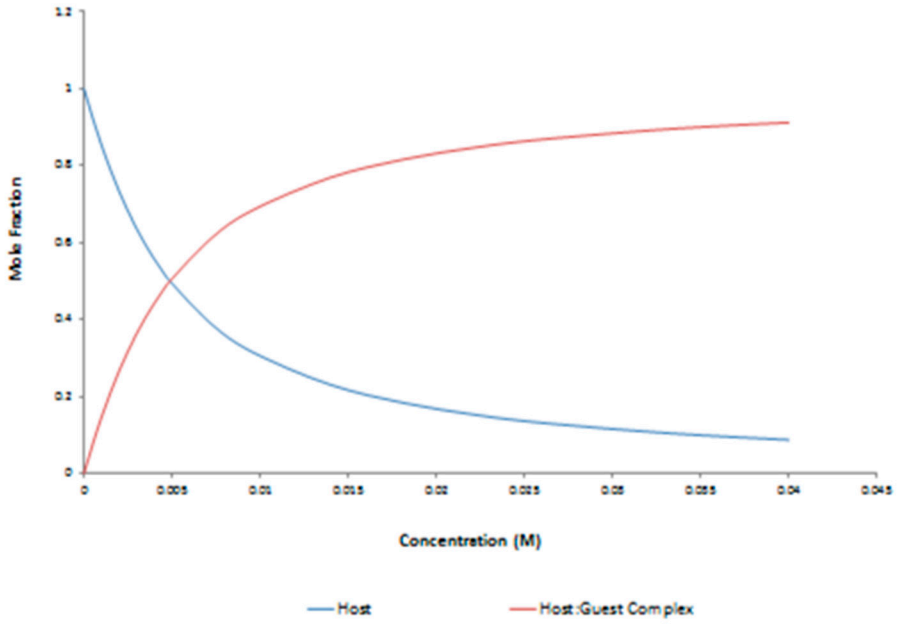

Figure S20: **(a)**: Bind fit graph of the ^{1}H NMR spectrum (chemical shift of Ha proton (ppm)) of **SN1** with increasing TBA chloride concentration in DMSO-d_6. **(b)**: Speciation graph of the ^{1}H NMR spectrum (chemical shift of Ha proton (ppm)) of **SN1** with increasing TBA chloride concentration in DMSO-d_6.

(a)

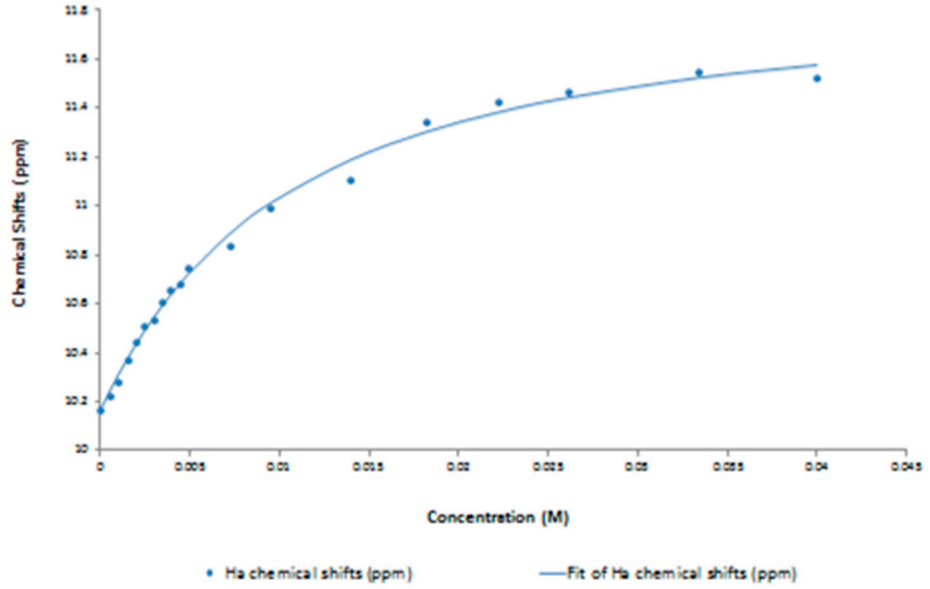

(b)

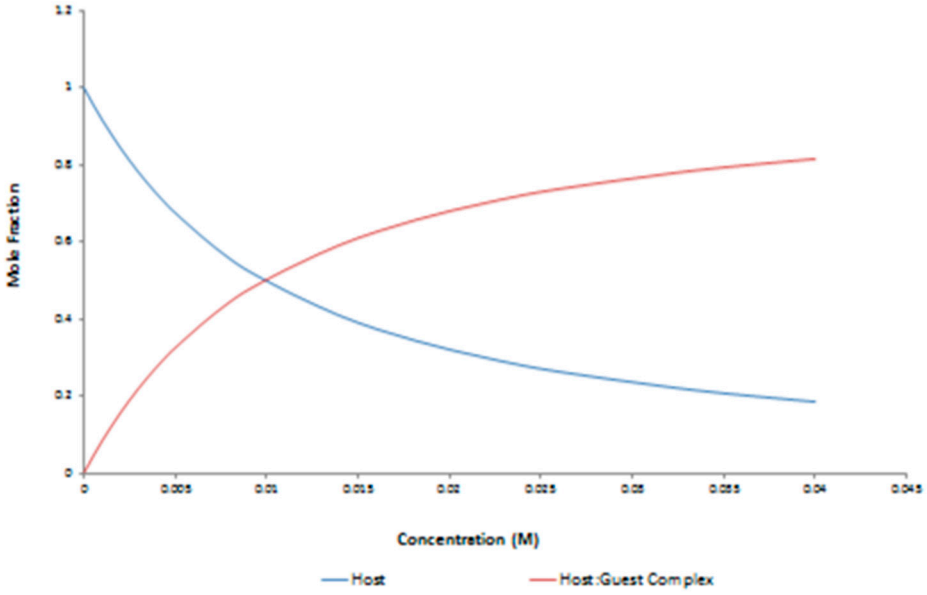

Figure S21: **(a)**: Bind fit graph of the ^{1}H NMR spectrum (chemical shift of Ha proton (ppm)) of **SN2** with increasing TBA chloride concentration in DMSO-d_6. **(b)**: Speciation graph of the ^{1}H NMR spectrum (chemical shift of Ha proton (ppm)) of **SN2** with increasing TBA chloride concentration in DMSO-d_6.

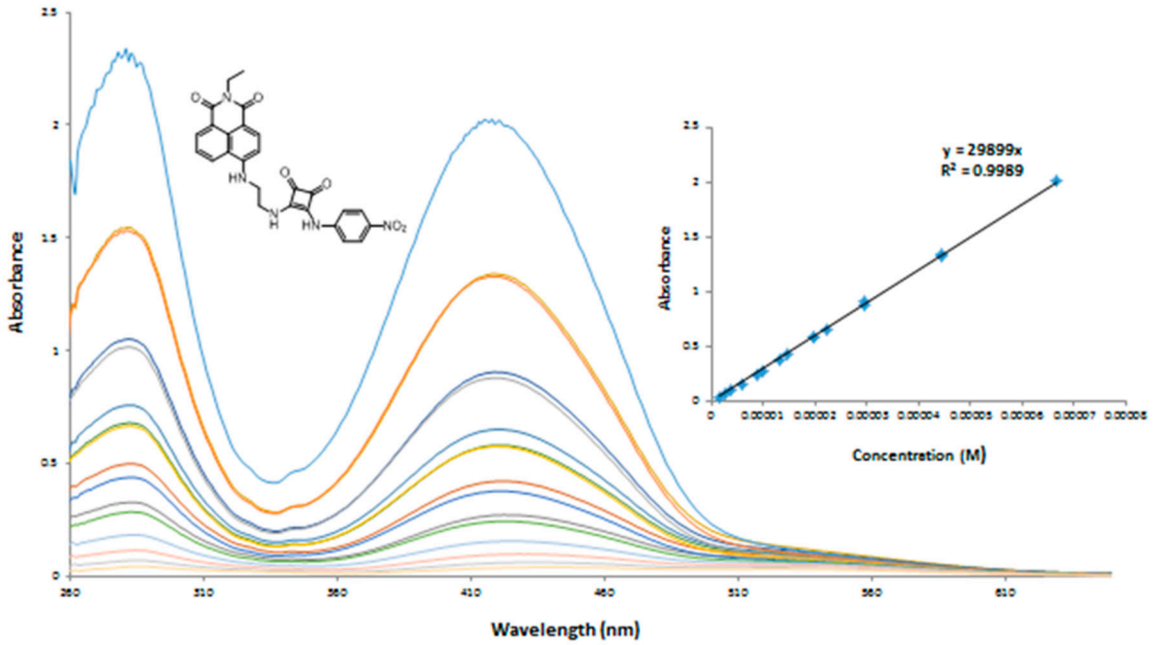

Figure S22: Changes in UV/Visible spectra upon increasing concentration of **SN1** in DMSO. **Insets:** Plots of absorbance at 420 nm as a function of increasing concentration of **SN1**.

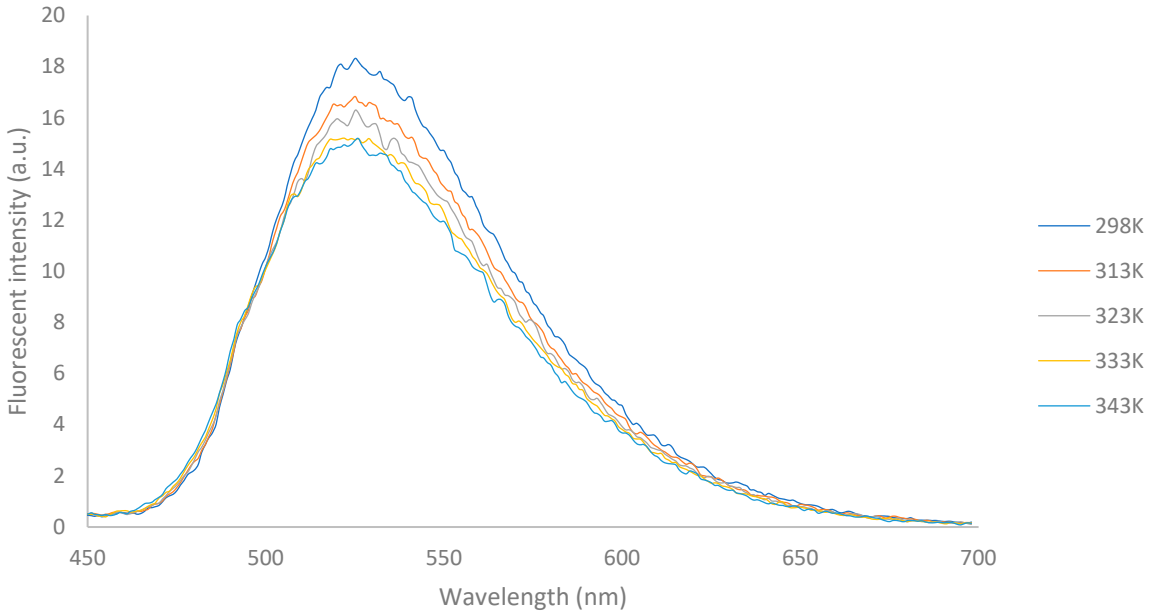

Figure S23: Changes in fluoresence spectrum of **SN1** as a function of temperature 298 K – 343 K in 5% aq. DMSO.

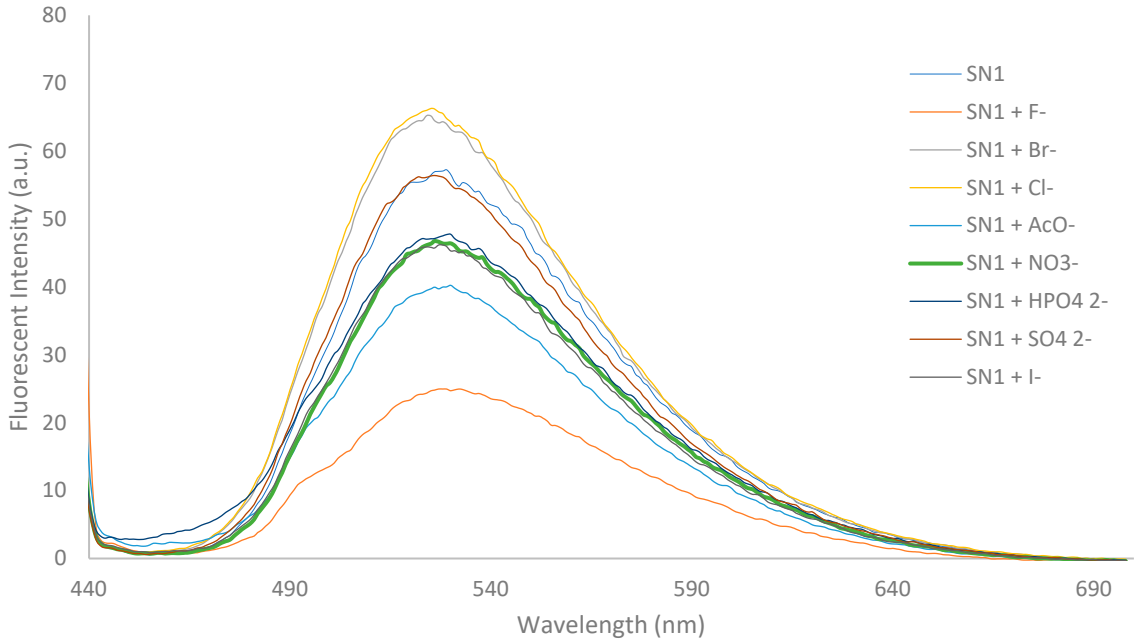

Figure S24: Changes in the fluorescence emission spectrum of **SN1** (λ_{ex} 430 nm) in DMSO with 20mM solution of different anions as TBA salts in DMSO (AcO^-, Cl^-, F^-, Br^-, I^-, NO_3^- HPO_4^{2-}, SO_4^{2-}).

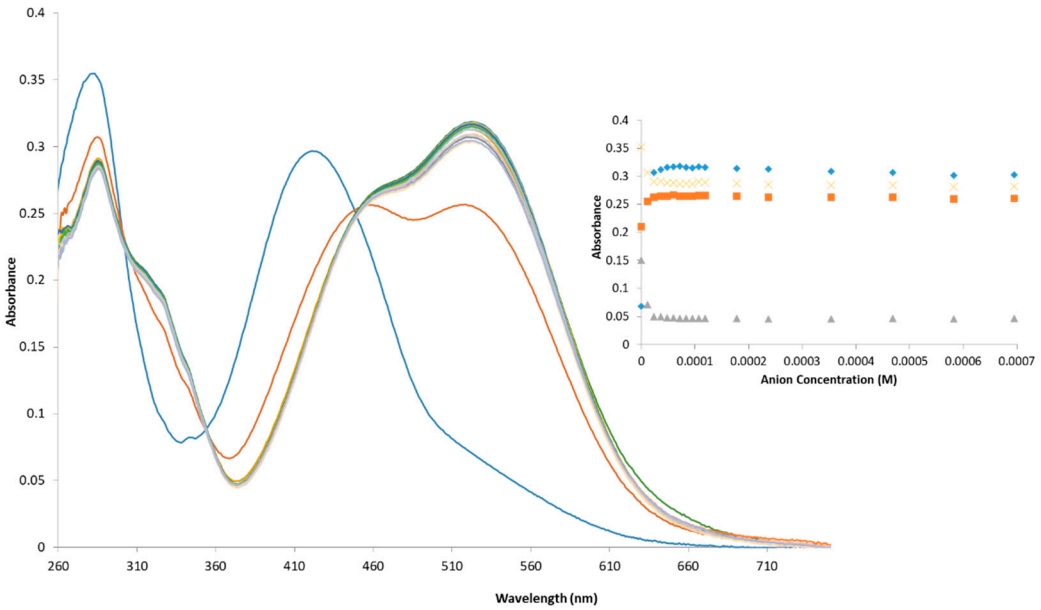

Figure S25: Changes in the UV/Visible spectrum of **SN1** (11.9µM) with increasing TBA acetate concentration in DMSO. **Insets:** Plots of the change in absorbance at 285 nm (yellow), 460 nm (orange), 375 nm (grey) and 525 nm (blue) as a function of TBA acetate concentration.

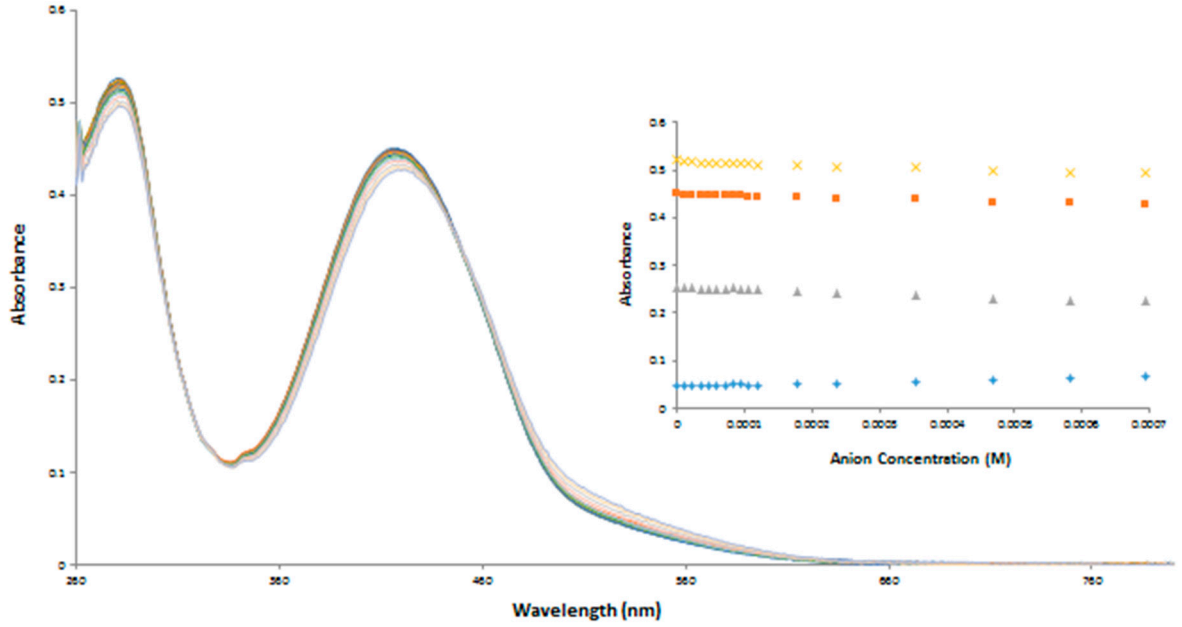

Figure S26: Changes in the UV/Visible spectrum of **SN1** (11.9µM) with increasing TBA chloride concentration in DMSO. **Insets:** Plots of the change in absorbance at 285 nm (yellow), 420 nm (orange), 375 nm (grey) and 525 nm (blue) as a function of TBA chloride concentration.

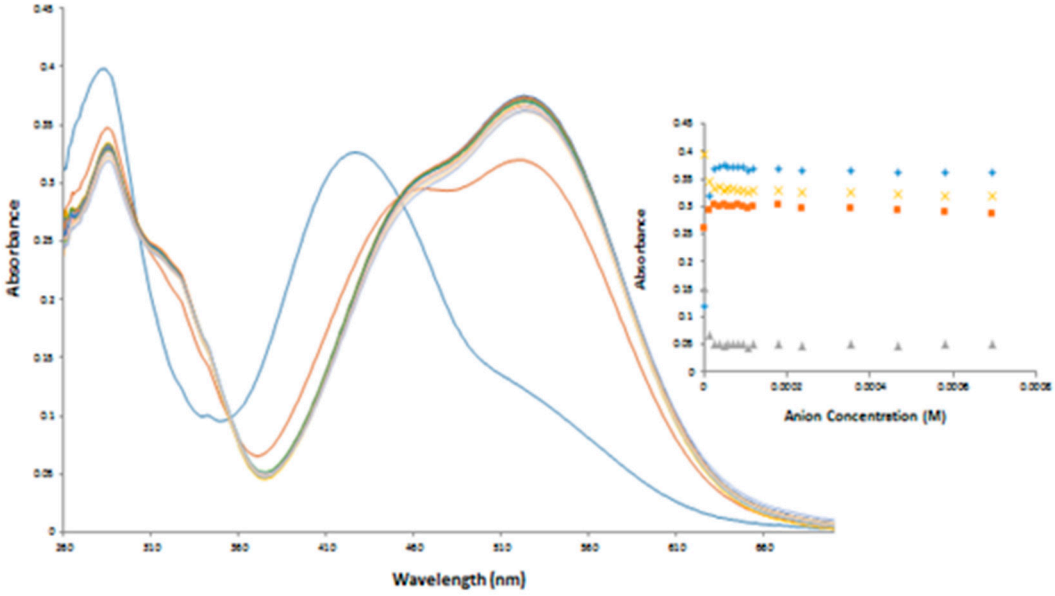

Figure S27: Changes in the UV/Visible spectrum of **SN1** (11.9µM) with increasing TBA fluoride concentration in DMSO. Plots of the change in absorbance at 285 nm (yellow), 460 nm (orange), 375 nm (grey) and 525 nm (blue) as a function of TBA fluoride concentration.

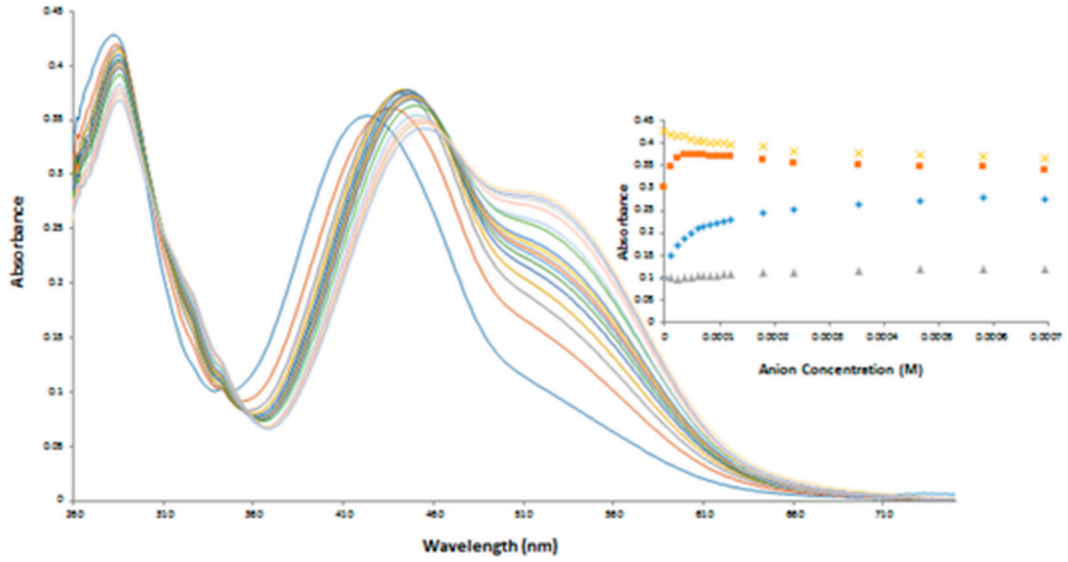

Figure S28: Changes in the UV/Visible spectrum of **SN1** (11.9µM) with increasing TBA phosphate concentration in DMSO. **Insets:** Plots of the change in absorbance at 285 nm (yellow), 450 nm (orange), 345 nm (grey) and 525 nm (blue) as a function of TBA phosphate concentration.

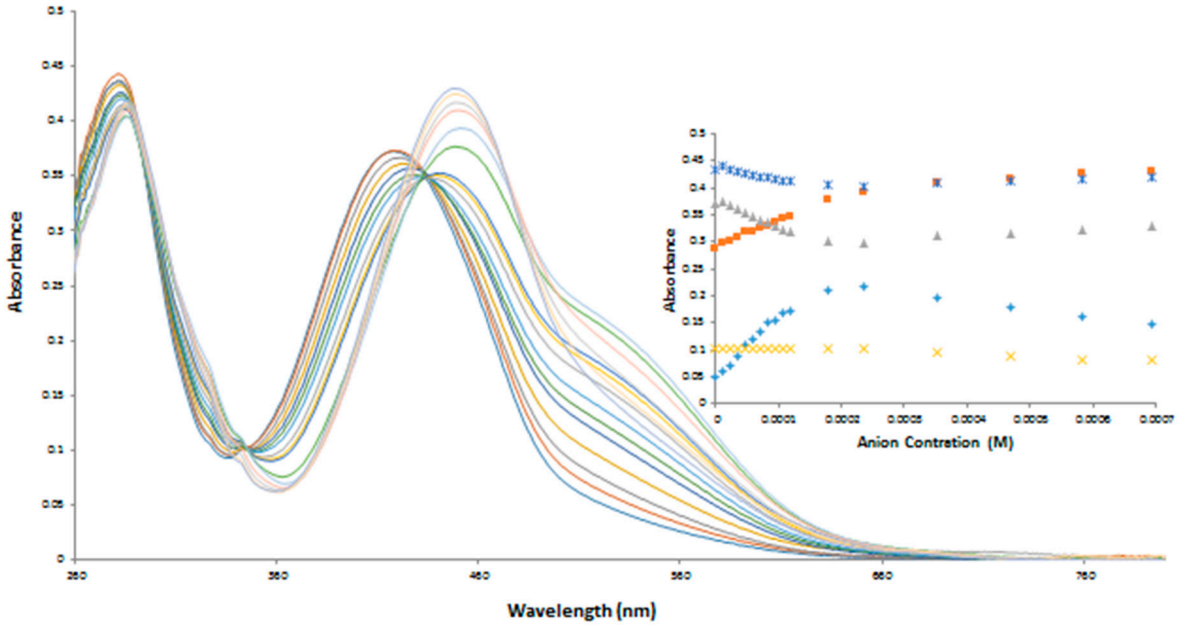

Figure S29: Changes in the UV/Visible spectrum of **SN1** (11.9µM) with increasing TBA sulfate concentration in DMSO. **Insets:** Plots of the change in absorbance at 285 nm (dark blue), 420 nm (grey), 450 nm (orange), 345 nm (yellow) and 525 nm (light blue) as a function of TBA sulphate concentration.

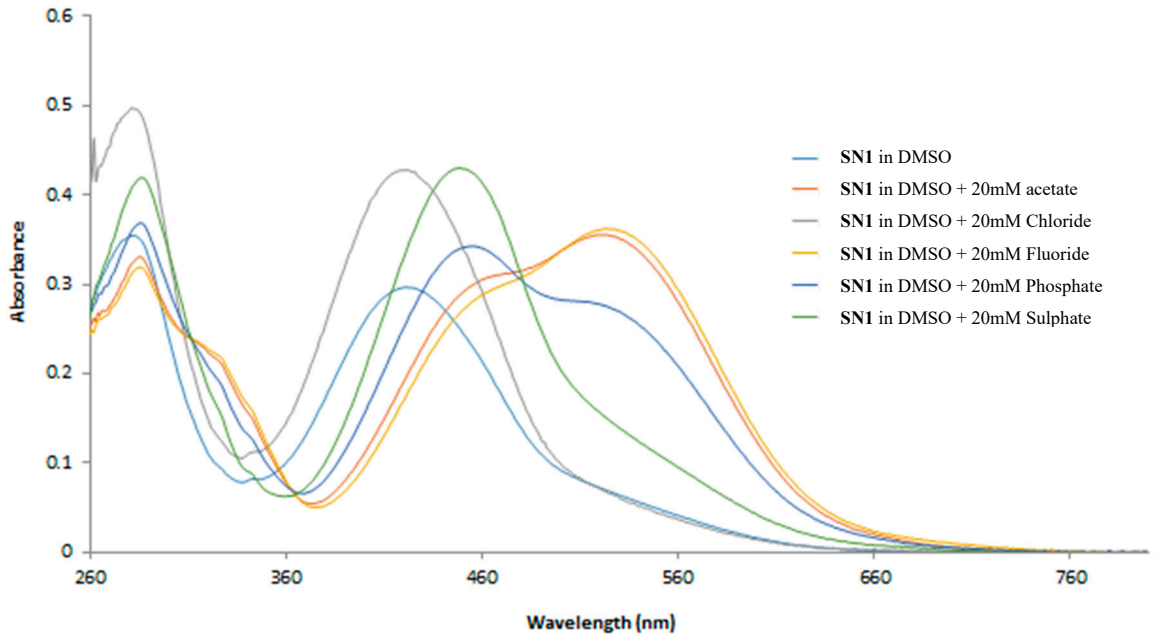

Figure S30: Changes in the UV/Visible spectrum of **SN1** (11.9µM) in DMSO with solution of different anions as TBA salts (20mM) in DMSO(AcO^-, Cl^-, F^-, PO_4^{3-}, SO_4^{2-}).

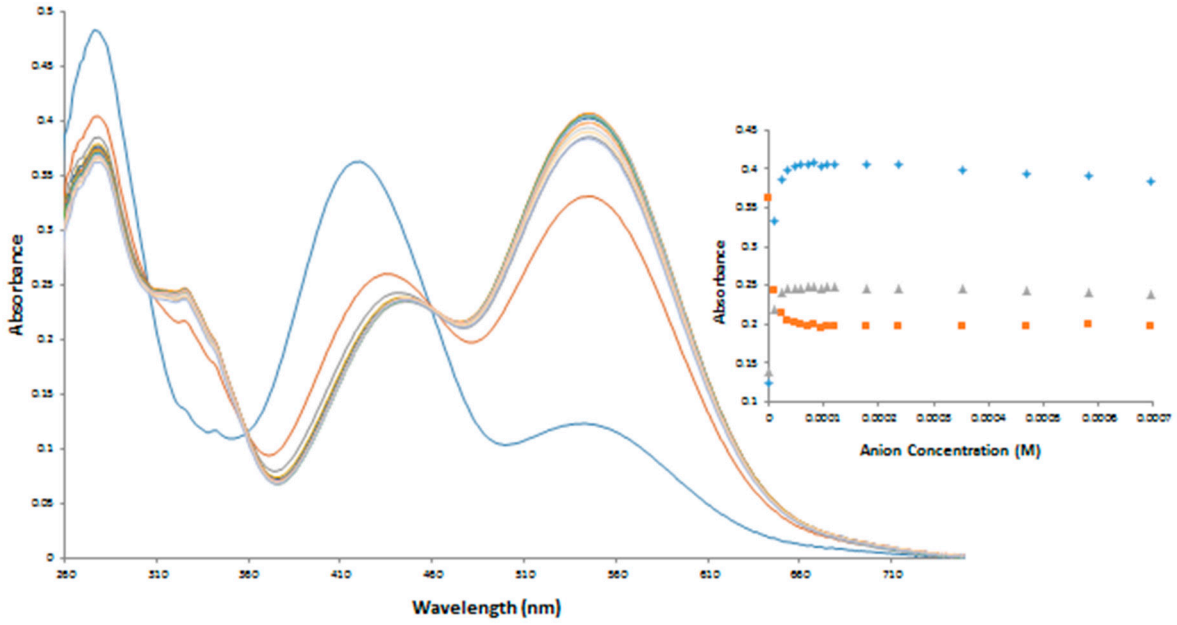

Figure S31: Changes in the UV/Visible spectrum of **SN2** (11.9µM) with increasing TBA acetate concentration in DMSO. **Insets:** Plots of the change in absorbance at 420 nm (orange), 325 nm (grey) and 545 nm (blue) as a function of TBA acetate concentration.

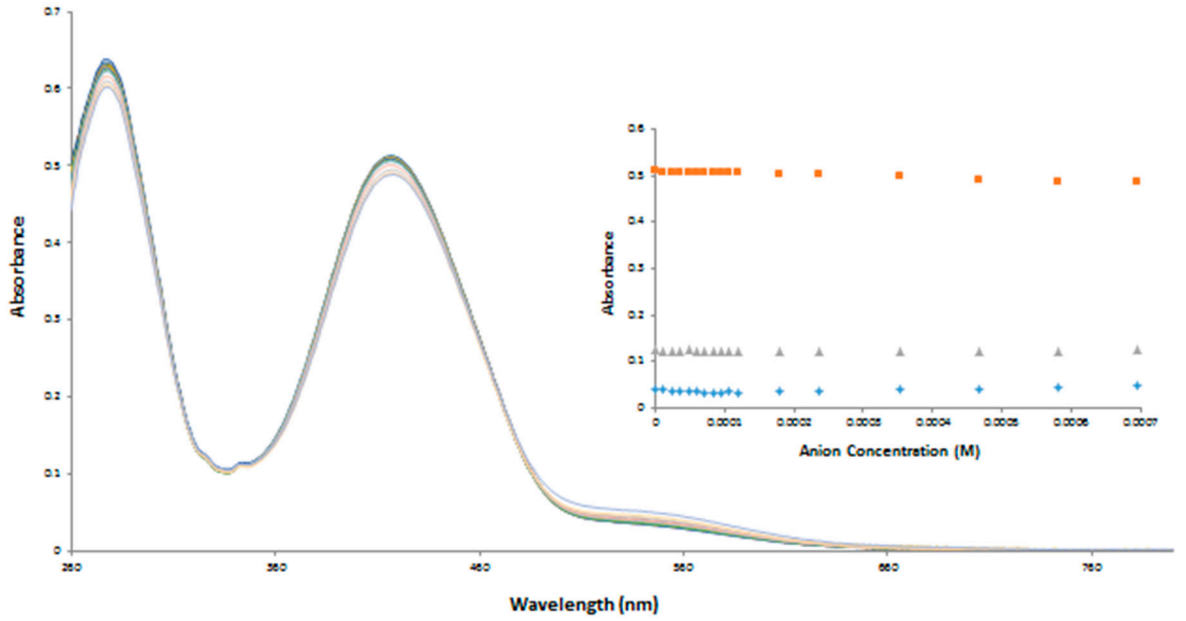

Figure S32: Changes in the UV/Visible spectrum of **SN2** (11.9µM) with increasing TBA chloride concentration in DMSO. **Insets:** Plots of the change in absorbance at 420 nm (orange), 325 nm (grey) and 545 nm (blue) as a function of TBA chloride concentration.

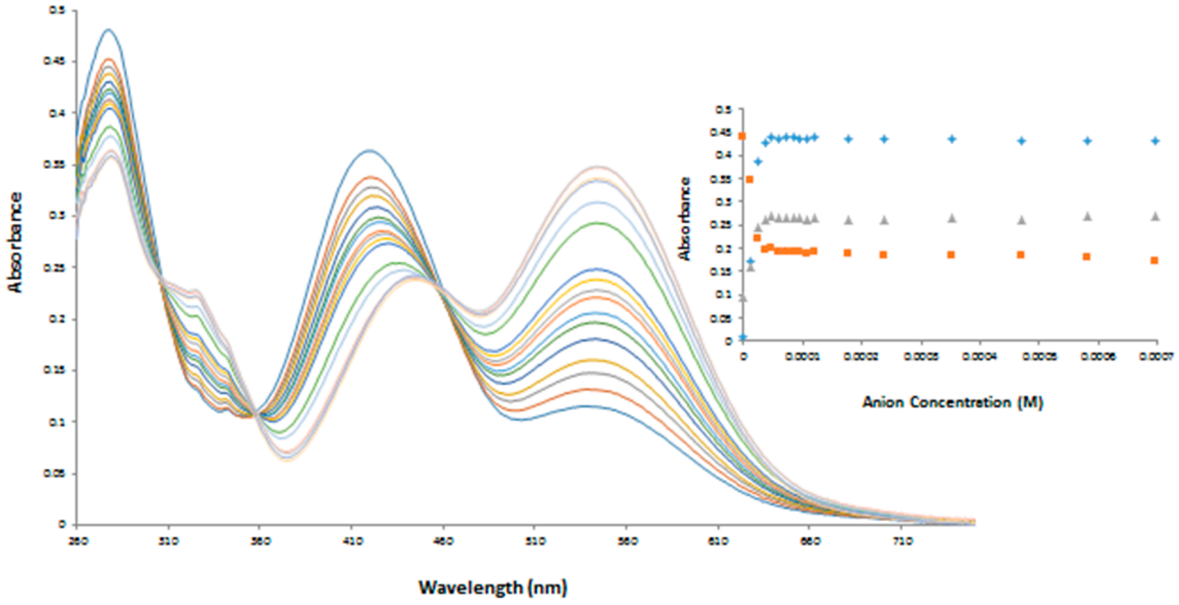

Figure S33: Changes in the UV/Visible spectrum of **SN2** (11.9µM) with increasing TBA fluoride concentration in DMSO. **Insets:** Plots of the change in absorbance at 420 nm (orange), 325 nm (grey) and 545 nm (blue) as a function of TBA fluoride concentration.

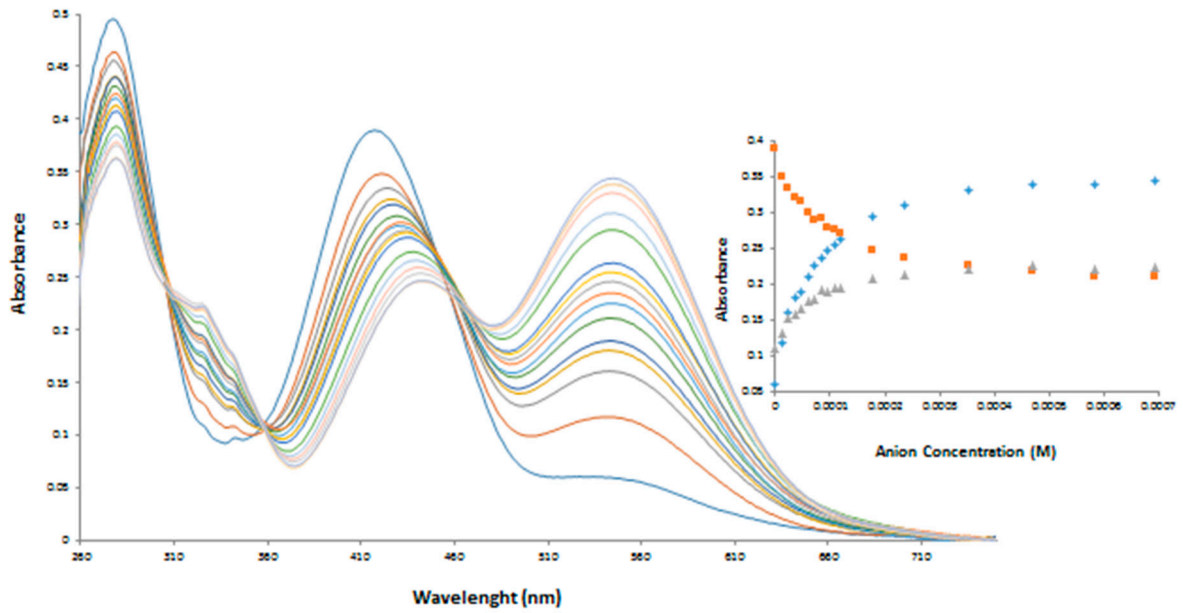

Figure S34: Changes in the UV/Visible spectrum of **SN2** (11.9µM) with increasing TBA phosphate concentration in DMSO. **Insets:** Plots of the change in absorbance at 420 nm (orange), 325 nm (grey) and 545 nm (blue) as a function of TBA phosphate concentration.

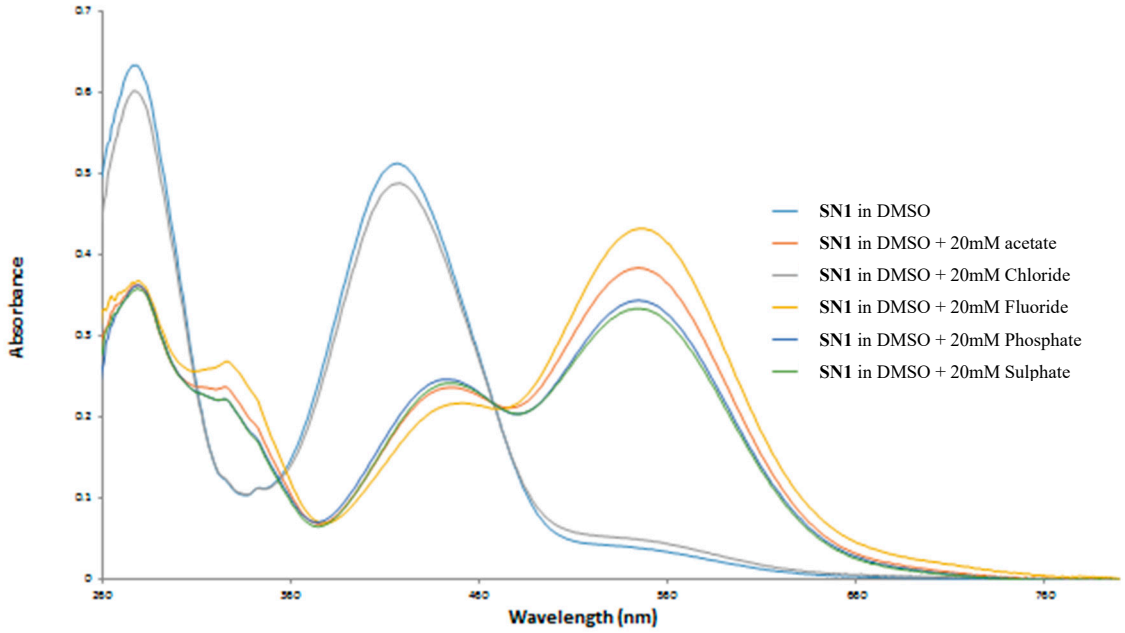

Figure S35: Changes in the UV/Visible spectrum of **SN2** (11.9µM) in DMSO with solution of different anions as TBA salts (20mM) in DMSO(AcO^-, Cl^-, F^-, PO_4^{3-}, SO_4^{2-}).

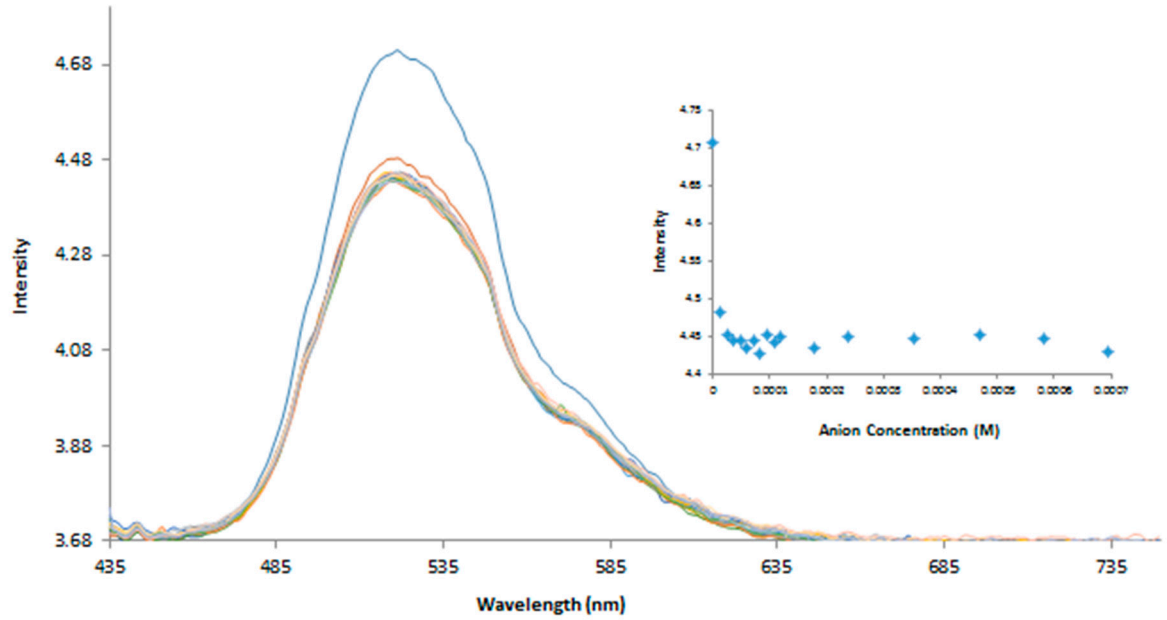

Figure S36: Changes in the fluorescence emission spectrum of **SN1** (λ_{ex} 430 nm) with increasing TBA acetate concentration in DMSO. **Insets:** Plots of the change in emission intensity at 522 nm as a function of TBA acetate concentration.

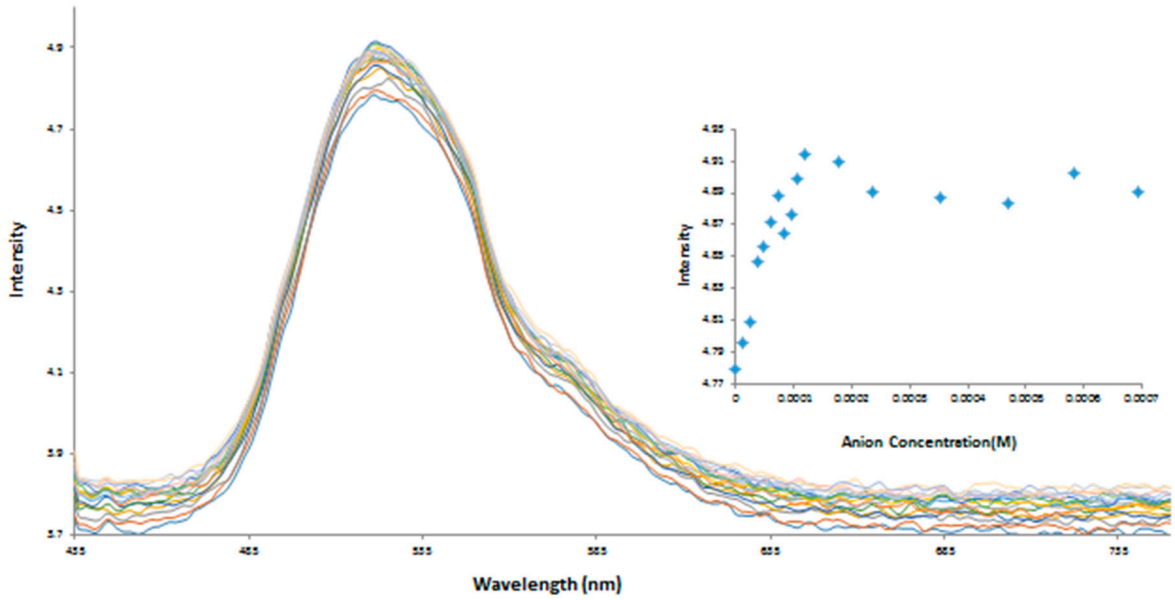

Figure S37: Changes in the fluorescence emission spectrum of **SN1** (λ_{ex} 430 nm) with increasing TBA chloride concentration in DMSO. **Insets:** Plots of the change in emission intensity at 522 nm as a function of TBA chloride concentration.

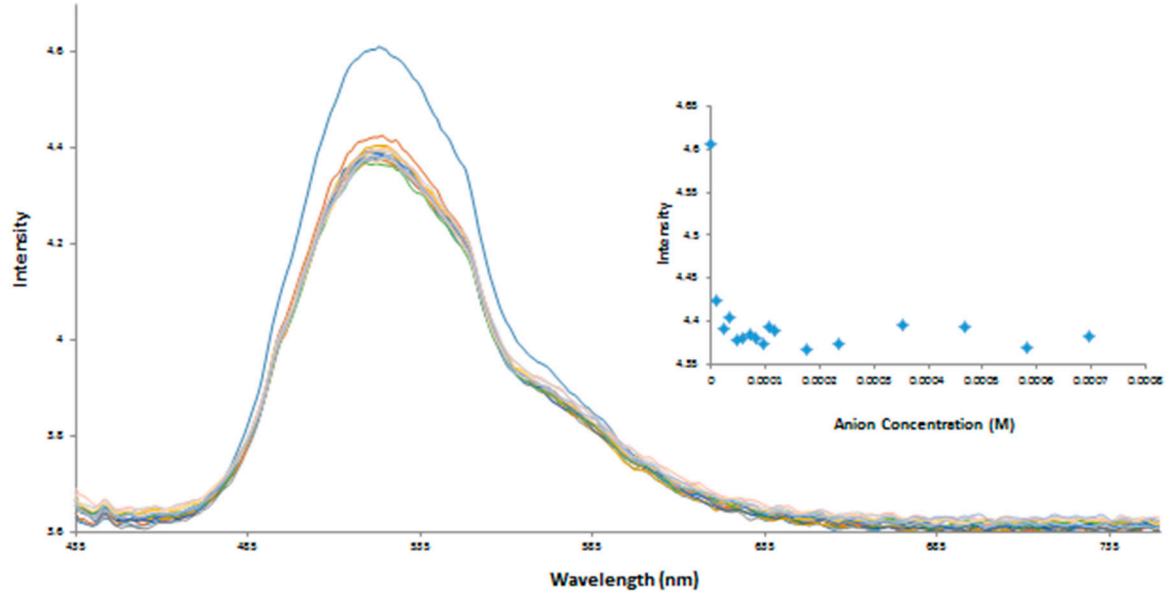

Figure S38: Changes in the fluorescence emission spectrum of **SN1** (λ_{ex} 430 nm) with increasing TBA fluoride concentration in DMSO. **Insets:** Plots of the change in emission intensity at 522 nm as a function of TBA fluoride concentration.

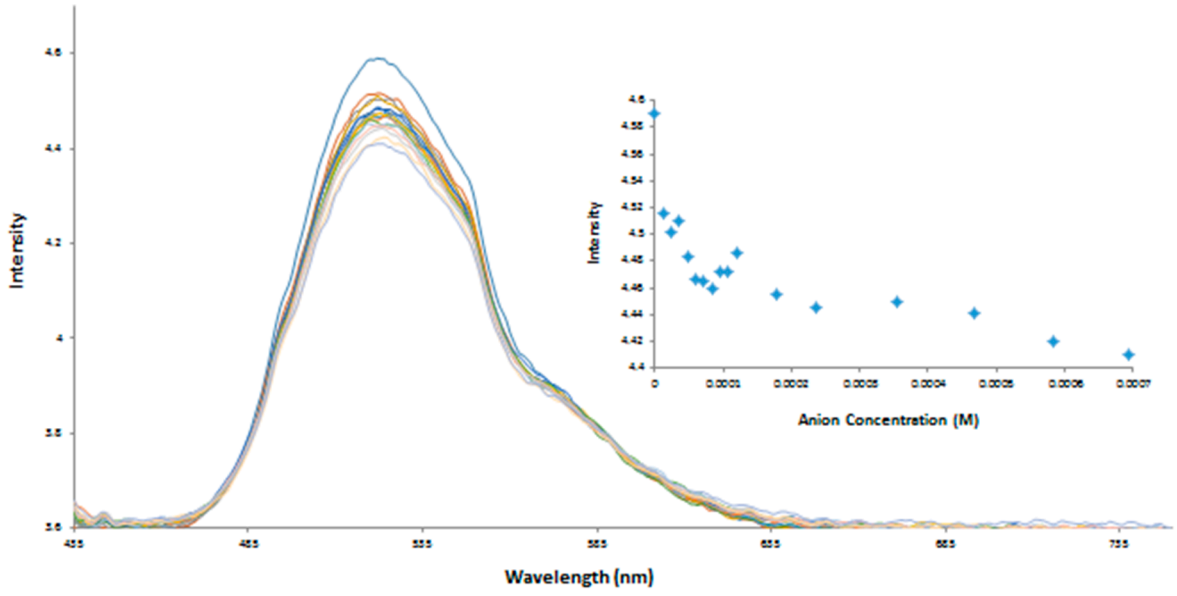

Figure S39: Changes in the fluorescence emission spectrum of **SN1** (λ_{ex} 430 nm) with increasing TBA phosphate concentration in DMSO. **Insets:** Plots of the change in emission intensity at 522 nm as a function of TBA phosphate concentration.

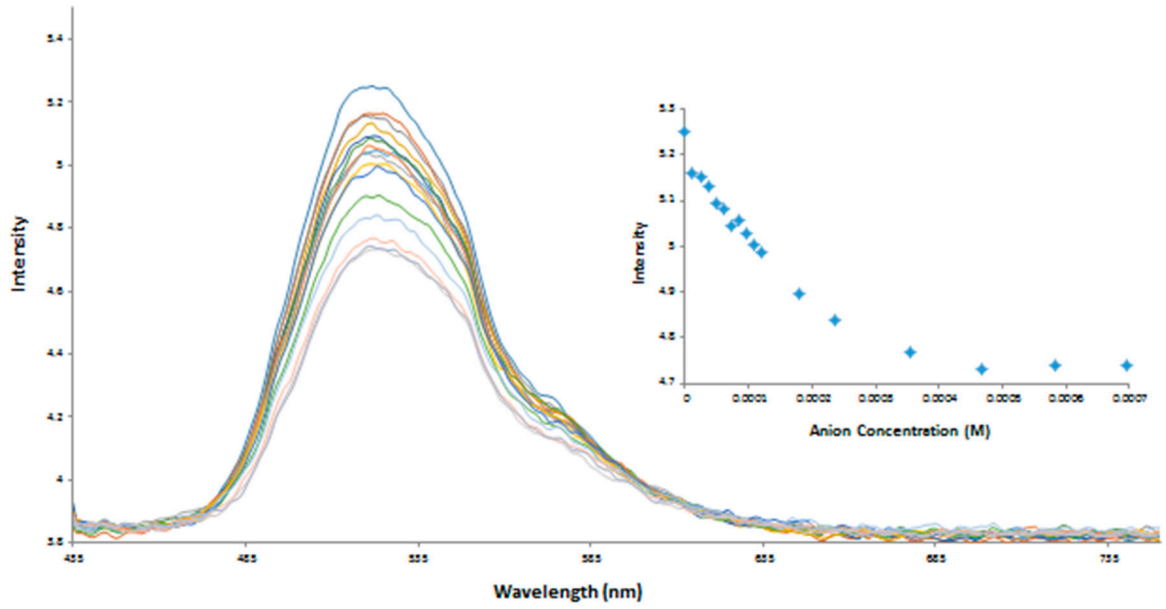

Figure S40: Changes in the fluorescence emission spectrum of **SN1** (λ_{ex} 430 nm) with increasing TBA sulphate concentration in DMSO. **Insets:** Plots of the change in emission intensity at 522 nm as a function of TBA sulphate concentration.

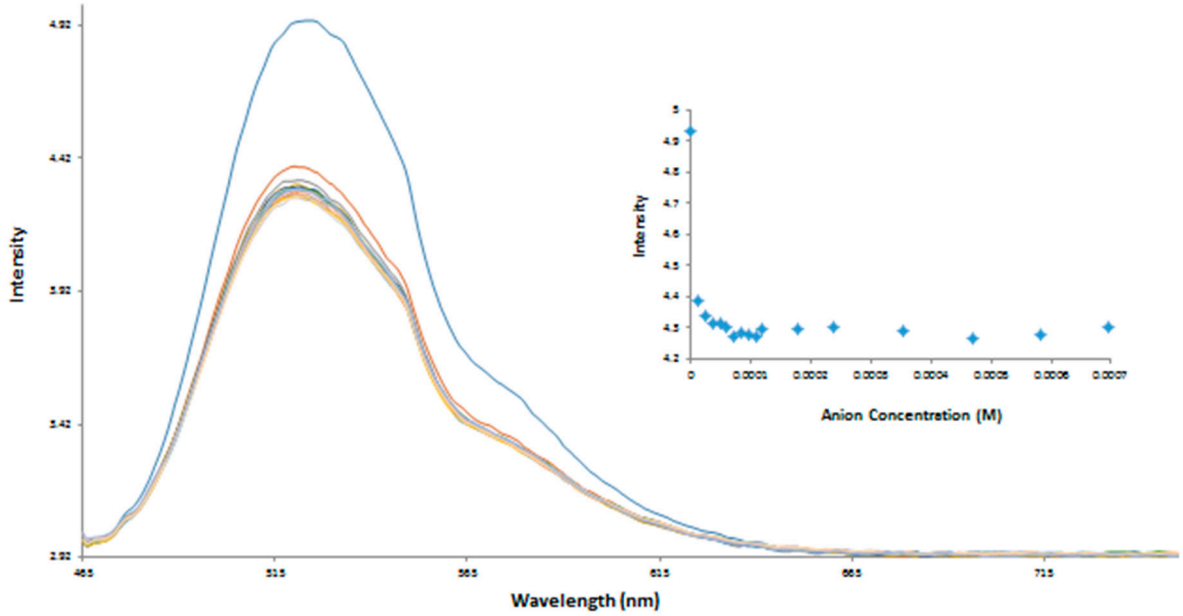

Figure S41: Changes in the fluorescence emission spectrum of **SN2** (λ_{ex} 460 nm) with increasing TBA acetate concentration in DMSO. **Insets:** Plots of the change in emission intensity at 522 nm as a function of TBA acetate concentration.

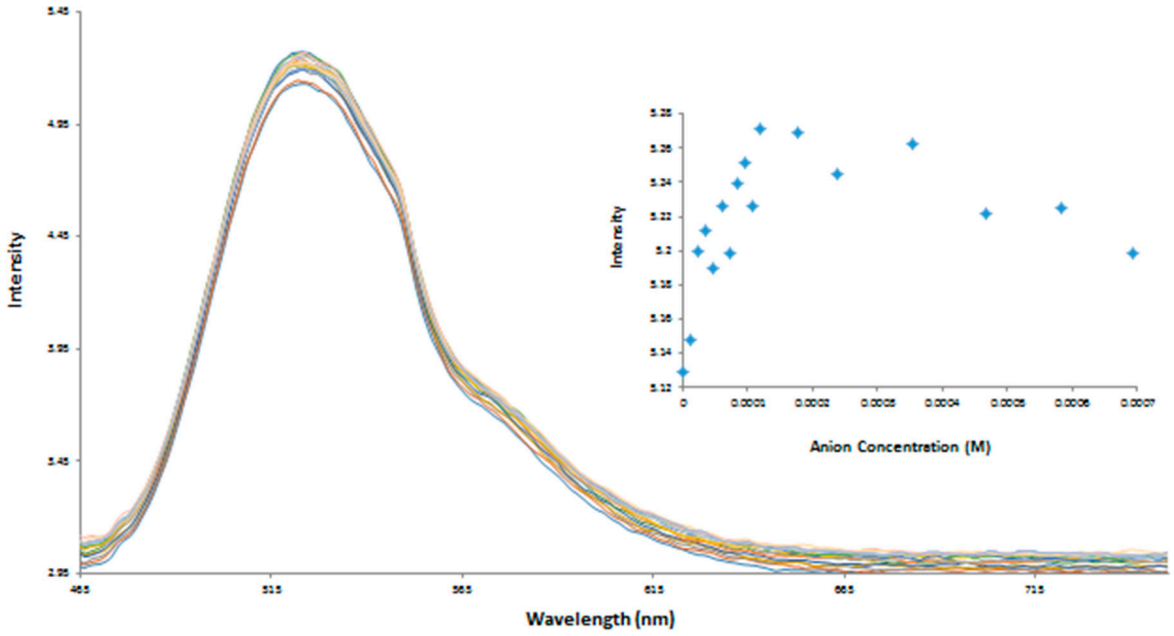

Figure S42: Changes in the fluorescence emission spectrum of **SN2** (λ_{ex} 460 nm) with increasing TBA chloride concentration in DMSO. **Insets:** Plots of the change in emission intensity at 522 nm as a function of TBA chloride concentration.

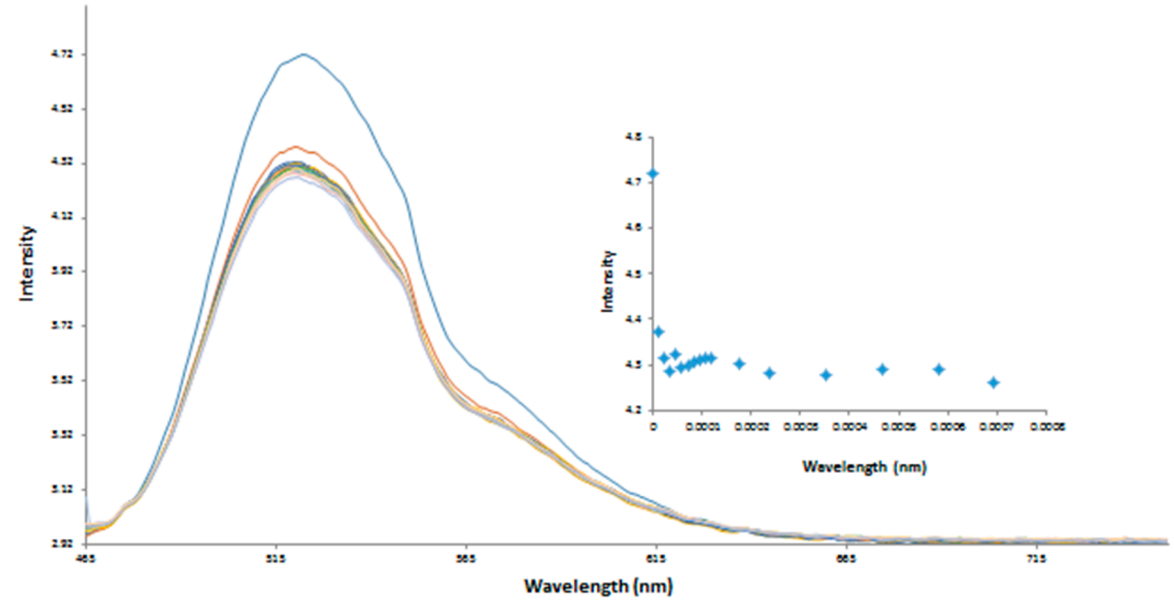

Figure S43: Changes in the fluorescence emission spectrum of **SN2** (λ_{ex} 460 nm) with increasing TBA fluoride concentration in DMSO. **Insets:** Plots of the change in emission intensity at 522 nm as a function of TBA fluoride concentration.

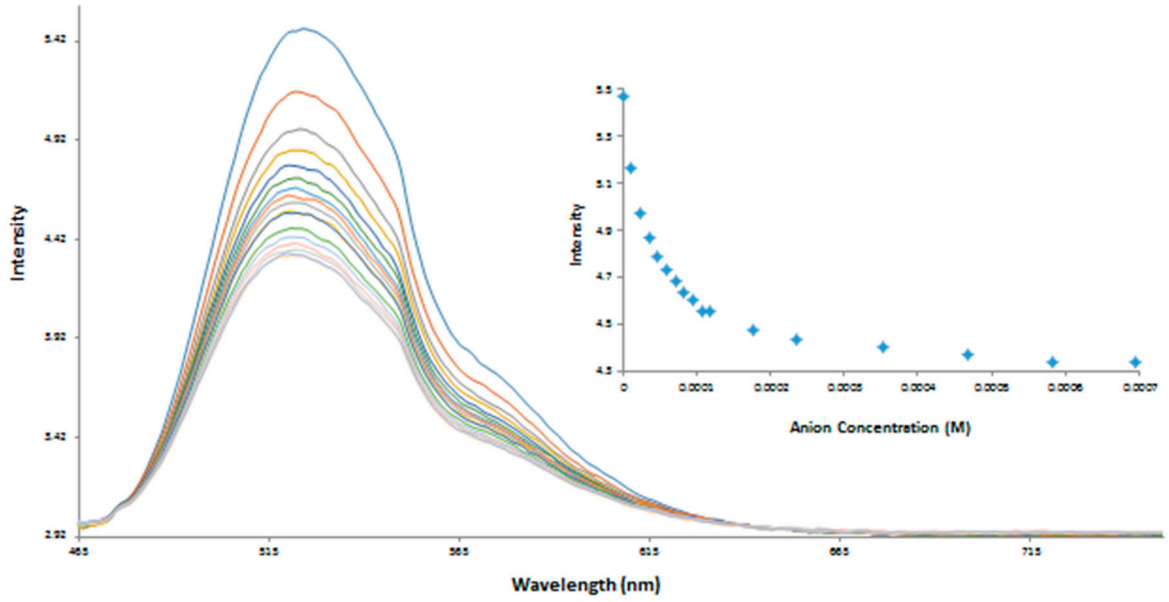

Figure S44: Changes in the fluorescence emission spectrum of **SN2** (λ_{ex} 460 nm) with increasing TBA phosphate concentration in DMSO. **Insets:** Plots of the change in emission intensity at 522 nm as a function of TBA phosphate concentration.

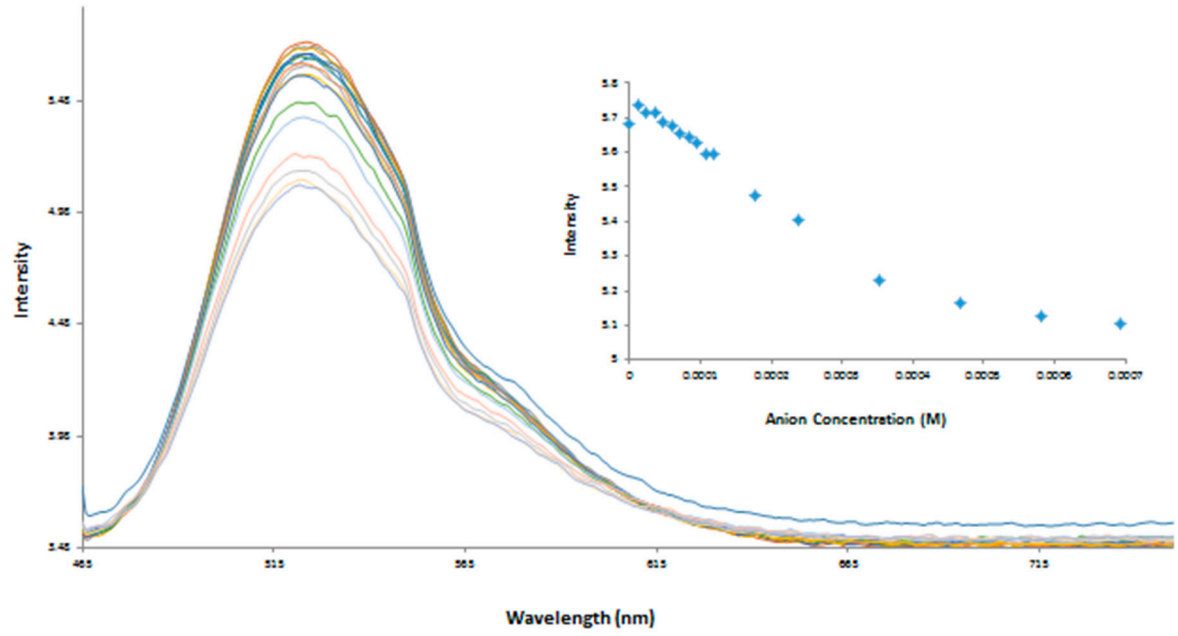

Figure S45: Changes in the fluorescence emission spectrum of **SN2** (λ_{ex} 460 nm) with increasing TBA sulphate concentration in DMSO. **Insets:** Plots of the change in emission intensity at 522 nm as a function of TBA sulphate concentration.

Table S1: Absorption properties of **SN1** and **SN2**

Receptor	λ_{max}(nm) [$\varepsilon(M^{-1}cm^{-1})$ in DMSO (3ml)	
	π- π^*	ICT
SN1	280 [34375]	420 [29899]
SN2	280 [35187]	420 [27410]